

Sequestered Dark Matter

B. v. Harling and A. Hebecker

*Institut für Theoretische Physik, Universität Heidelberg, Philosophenweg 16 und 19,
D-69120 Heidelberg, Germany*

(harling and a.hebecker@thphys.uni-heidelberg.de)

Abstract

We show that hidden-sector dark matter is a generic feature of the type IIB string theory landscape and that its lifetime may allow for a discovery through the observation of very energetic γ -rays produced in the decay. Throats or, equivalently, conformally sequestered hidden sectors are common in flux compactifications and the energy deposited in these sectors can be calculated if the reheating temperature of the standard model sector is known. Assuming that throats with various warp factors are available in the compact manifold, we determine which throats maximize the late-time abundance of sequestered dark matter. For such throats, this abundance agrees with cosmological data if the standard model reheating temperature was $10^{10} - 10^{11}$ GeV. In two distinct scenarios, the mass of dark matter particles, i.e. the IR scale of the throat, is either around 10^5 GeV or around 10^{10} GeV. The lifetime and the decay channels of our dark matter candidates depend crucially on the fact that the Klebanov-Strassler throat is supersymmetric. Furthermore, the details of supersymmetry breaking both in the throat and in the visible sector play an essential role. We identify a number of scenarios where this type of dark matter can be discovered via γ -ray observations.

1 Introduction

Dark matter is frequently assumed to consist of massive weakly interacting particles which are stable (or have a very long lifetime) because their decay is forbidden by some (approximate) symmetry. However, it is also well-known that dark matter may originate in a hidden sector which is coupled to the standard model only via higher-dimension operators, ensuring that dark matter does not decay (see e.g. [1, 2]).

We demonstrate that the latter scenario is realized under fairly general assumptions in the type IIB string theory landscape. The main starting point is the well-known fact that type IIB flux compactifications generically contain many strongly warped regions or throats [3]. This statement can be made quantitative [4] under the assumption that the fine-tuning of the cosmological constant requires manifolds with many 3-cycles and that, in many cases, such 3-cycles produce Klebanov-Strassler throats [5] if stabilized at small volume. We do not assume that inflation is realized in one of these throats but base our analysis only on the fact that, after inflation ends, the standard model sector is heated to a certain temperature. Moreover, we assume that the throats have received no energy from the reheating process.¹ Even under such minimal assumptions, a certain amount of energy is deposited in the various throats by energy transfer from the heated standard model sector. There exist certain optimal throat lengths (i.e. optimal warp factors) for which a given throat contains a maximal amount of cold dark matter in the late universe. Requiring furthermore that such an ‘optimal’ throat is responsible for the dark matter observed today, we determine the reheating temperature to be between 10^{10} GeV and 10^{11} GeV. The IR scale of the relevant throat (i.e. the mass of dark matter particles) is either around 10^5 GeV or around 10^{10} GeV.

The fact that dark matter can come from a hidden (or more precisely conformally sequestered) sector realized by a Klebanov-Strassler throat has already been emphasized in [6]. We approach this possibility from a more general perspective (without relying on either the standard model or inflation being realized in warped regions) and perform a quantitative analysis based on the assumption that various throats may be available. It turns out that supersymmetry, being a fundamental feature both of the underlying 10d theory as well as of the Klebanov-Strassler solution, plays a central role in the phenomenology of sequestered dark matter. Furthermore, our numerical results differ from previous estimates because we use our new values for the energy transfer rate between throats [7]. Finally, we observe that the decay rate of throat dark matter to the standard model sector is not negligible. It may, for a certain range of parameters, lead to the discovery of this variant of dark matter via the observation of the diffuse γ -ray background or the spectrum of very energetic γ -rays.

Our paper is organized as follows: Sect. 2 describes the thermal production of sequestered dark matter. Using the energy transfer rates from [7], we determine the energy density deposited in a throat by the heated standard model sector. We show that the Kaluza-Klein (KK) modes which are produced in that way thermalize for a certain range

¹ Alternatively, if this assumption is not fulfilled, i.e. if the throats are heated directly by the reheating mechanism, a lower reheating temperature would be sufficient for our scenario.

of parameters. Whether this happens or not influences the further time evolution of the energy density significantly. Taking this into account, we calculate the late-time abundance of KK modes as a function of the reheating temperature and the IR scale of the throat. In Sect. 3, we discuss various decay channels of the KK modes. We show that they decay very quickly to a scalar state and its fermionic superpartner. These lightest KK modes can then decay to the standard model sector. We determine the corresponding decay rates which turn out to be different for the scalar and the fermion. Cosmological scenarios are discussed in Sect. 4. First, we analyse setups with a single throat. We find that a moderately long throat gives a promising dark matter candidate which may allow for a discovery by upcoming γ -ray experiments. Then, we consider scenarios with a large number of throats, using results on the distribution of multi-throat configurations from [4]. We find that a throat of the required length is in many cases present. Some issues concerning supersymmetry breaking in the throat sector are discussed in Sect. 5. Finally, in Sect. 6, we give a summary of our results.

2 Thermal production

2.1 Energy transfer

As outlined in the Introduction, we assume the throats to have received no energy from the reheating process, whereas the standard model is heated to a temperature T_{RH} initially. Subsequently, energy will be transferred from the standard model to the throats. Note that this process is similar to the energy transfer from the hot brane to the bulk in Randall-Sundrum II models [8] (see also [9]). The AdS₅ bulk plays the role of the throat, which we however assume to be of finite length, with the Klebanov-Strassler region corresponding to the IR brane.

In [7], we have estimated the energy transfer rate between a heated Klebanov-Strassler (KS) throat at temperature T and another throat in a type IIB flux compactification. Our estimate is based on a calculation which can be performed in a simpler setting: two AdS₅ × S⁵ throats embedded in a 6d torus. For the purpose of this analysis, we have replaced the throats by equivalent stacks of D3-branes. In this language, the aforementioned energy transfer is that from a heated gauge theory living on one brane stack via supergravity fields in the embedding torus to the gauge theory living on the other brane stack. The coupling of supergravity in the torus to the gauge theories on the two brane stacks follows from the DBI action. Performing a KK expansion of the supergravity fields, the calculation of the energy transfer rate becomes a simple exercise in quantum field theory. One finds

$$\dot{\rho} \sim \frac{N_1^2 N_2^2}{M_{10}^{16} A^8} T^{13} + \frac{N_1^2 N_2^2}{M_{10}^{16} L^{12}} T^9, \quad (1)$$

where M_{10} is the 10d Planck scale, A is the distance between the two brane stacks/throats and L is the size of the embedding torus. Moreover, N_1 and N_2 are the numbers of

branes of the two stacks. The world-volume theories then have $\sim N_1^2$ and $\sim N_2^2$ degrees of freedom, respectively.

This energy transfer rate is also applicable to our setup. To this end, instead of a heated throat, we consider some D3- and/or D7-brane-realization of the standard model (with $g \sim 100$ degrees of freedom). To account for this modification, we simply have to set $N_1^2 = g$ in Eq. (1). Moreover, instead of an $\text{AdS}_5 \times \text{S}^5$ throat we are interested in energy transfer to a KS throat. The equivalent description is that of a stack of D3- and fractional D3-branes at a conifold singularity. For the absorption process, the relevant part of the geometry is the UV end of the throat, which is well approximated by $\text{AdS}_5 \times \text{T}^{1,1}$. This in turn is equivalent to a large number of D3-branes at a conifold singularity, which we denote by N_{UV} since it corresponds to the number of 5-form flux at the UV end of the KS throat. Therefore, $N_2 = N_{\text{UV}}$ in Eq. (1). We assume that the temperature of the standard model is smaller than the compactification scale, i.e. $T < L^{-1}$. Moreover, we consider the generic situation that the distance between the two brane stacks is of the same order of magnitude as the size of the embedding manifold, i.e. $A \sim L$. In this case, the second term in Eq. (1) dominates.² As explained in [7], this term is due to the effect of the zero mode in the KK expansion of supergravity fields and is therefore completely insensitive to the unknown details of the Calabi-Yau geometry. In [7], we focused on the dilaton, which is one of the supergravity fields mediating the energy transfer. However, using the coupling of the 10d graviton to the energy-momentum tensors on the two brane stacks, Eq. (1) can also be derived on the basis of the graviton as the mediating field. Since the zero mode of the dilaton acquires a mass in flux compactifications à la GKP [10], its effect is suppressed in this case. We therefore focus on the graviton zero mode as the field responsible for the second term in Eq. (1).

Using the relation $M_4 \sim M_{10}^4 L^3$ for the 4d Planck scale, the energy transfer rate is given by

$$\dot{\rho} \sim g N_{\text{UV}}^2 \frac{T^9}{M_4^4}. \quad (2)$$

This rate is easily understood as being due to a gravitational strength coupling between a sector with g degrees of freedom (the standard model) and a sector with N_{UV}^2 degrees of freedom (the KS throat).

The finite length of the KS throat implies the existence of an IR scale m_{IR} , the mass of the lowest-lying KK mode in the throat. In the dual picture, this corresponds to the fact that the fractional D3-branes break conformal invariance and induce a confinement or IR scale m_{IR} in the gauge theory. Thus, KK modes in the throat (i.e. glueballs of the dual gauge theory) can only be created if $T_{\text{RH}} > m_{\text{IR}}$. We then expect these glueballs to have masses up to $m \sim T_{\text{RH}}$.

The glueballs may decay back to the standard model. Jumping somewhat ahead, we

² All subsequent results are easily extended to the case of nearby throats by simply using the first instead of the second term in Eq. (1) and performing an analogous modification of the dark matter decay rates.

note that spin-2 glueballs have the highest decay rate (see Sect. 3.2 for details):

$$\Gamma(m) \sim g N_{\text{UV}}^2 \frac{m^4 m_{\text{IR}}}{M_4^4}. \quad (3)$$

On the other hand, glueballs can also decay to lighter glueballs within the same throat. We will have to discuss this process in some detail below. At the moment, it is sufficient to establish that the decay to lighter glueballs wins over the possible decay back to the standard model. For this purpose, we recall that we are dealing with a strongly coupled system with a dense spectrum. Thus, the initially created gauge theory state of mass m will have a lifetime $\sim 1/m$. In the most conservative scenario, it will decay to 2 states of mass $m/2$. These states will in turn decay to states of mass $m/2^2$ after a time-interval $\sim 2/m$, and so on. Summing up the probabilities for the decay back to the standard model at each step of this cascade, we arrive at a total probability

$$w \sim \sum \Gamma(m/2^n) \cdot \frac{2^n}{m}. \quad (4)$$

This sum is of the same order of magnitude as the first term and hence very small in all cases of interest. Clearly, we could equally well have assumed that each glueball decays to k_1 lighter states with mass m/k_2 , arriving at the same conclusion for any $\mathcal{O}(1)$ numbers k_1 and k_2 . Thus, the relaxation to lighter states within the same throat always wins over the decay back to the standard model or to other throats.

The energy transfer rate Eq. (2) is strongly temperature dependent, $\dot{\rho} \propto T^9$. Therefore, energy transfer is effectively finished soon after reheating and the corresponding time scale is $|T/\dot{T}|$ at $T = T_{\text{RH}}$. The total energy density after reheating is dominated by the relativistic gas in the standard model sector with $\rho = g \frac{\pi^2}{30} T^4$. We find

$$|T/\dot{T}| = H^{-1} \sim \frac{M_4}{g^{1/2} T^2}, \quad (5)$$

where H is the Hubble rate. Using Eqs. (2) and (5) at $T \sim T_{\text{RH}}$, the energy density deposited in a throat directly after reheating is

$$\rho \sim \dot{\rho} |T/\dot{T}| \sim g^{1/2} N_{\text{UV}}^2 \frac{T_{\text{RH}}^7}{M_4^3}. \quad (6)$$

Before closing this section, we note that the energy transfer processes we consider compete with the unavoidable energy deposition in the throat sectors occurring during inflation. This can be understood by noting that de Sitter space has a temperature $T_{\text{dS}} \sim 1/R_{\text{dS}} \sim M_{\text{Inf}}^2/M_4$. We assume that inflation lasts long enough for the throats to be thermalized with this temperature. Furthermore, parameterizing the efficiency of reheating by an efficiency factor $\epsilon \leq 1$, we have $g T_{\text{RH}}^4 \sim \epsilon M_{\text{Inf}}^4$. Thus, all throats have a temperature $T_{\text{dS}} \sim \sqrt{g/\epsilon} T_{\text{RH}}^2/M_4$ at the time of reheating. Jumping ahead, we note that for typical long throats (where this effect is most relevant), we find initial throat temperatures $\sim 10^6$ GeV and $T_{\text{RH}} \sim 10^{11}$ GeV. For such throats, ‘de-Sitter heating’ in fact wins over the heating process analysed in this section if $\epsilon < 1$, allowing in principle for even more throat dark matter than we find in our conservative analysis.

2.2 Time evolution of the energy density

The gauge theory states created by energy transfer from the standard model sector decay into a certain number of the lightest glueballs of mass m_{IR} with a certain distribution of kinetic energies. Two extremal cases are possible. In one case, the initial gauge theory state decays into an $\mathcal{O}(1)$ number of the lightest glueballs which accordingly have kinetic energies of the order of T_{RH} . In the other case, the initial gauge theory state settles into a large number of the lightest glueballs with kinetic energies of the order of their mass m_{IR} . In between these two extremal cases, a continuous distribution of kinetic energies is a priori possible. The knowledge of this distribution is important since it determines whether the glueballs can reach thermal equilibrium after reheating and whether (or for how long) the energy density scales like radiation or like matter with the expansion of the universe. This in turn determines how large the contribution of the glueballs to the total energy density is at our epoch. Since we are at present unable to determine this distribution of kinetic energies, we discuss the two extremal cases separately. This allows us to estimate the possible range of contributions of the glueballs to the current energy density of the universe as a function of the parameters m_{IR} , N_{UV} and T_{RH} .

We begin by collecting some results from the literature on the thermodynamics of the gauge theories that are relevant for our discussion. The gauge theory dual to a KS throat has a logarithmically varying number of degrees of freedom, corresponding to the logarithmic deviation of the KS geometry from AdS_5 . In the deconfined phase, the effective number of colours N_{eff} of the gauge theory depends on the temperature \tilde{T} of the plasma as

$$N_{\text{eff}} \sim N_{\text{IR}} \ln \left(\frac{\tilde{T}}{m_{\text{IR}}} \right). \quad (7)$$

Here, N_{IR} is the number of 5-form flux at the bottom of the throat. The deconfined phase of the gauge theory is dual to a throat with a black hole horizon which replaces the IR end. The highest meaningful value in Eq. (7) is $N_{\text{eff}} \sim N_{\text{UV}}$. This corresponds to a temperature where the black hole horizon reaches the UV end of the throat. The energy density as a function of the plasma temperature \tilde{T} is

$$\rho \sim N_{\text{eff}}^2 \tilde{T}^4. \quad (8)$$

Since the logarithmic variation of N_{eff} with \tilde{T} is small compared to the variation of the \tilde{T}^4 -term, we will neglect it in the following. The deconfined phase can then be described by an approximate conformal field theory and the energy density correspondingly scales like radiation with a^{-4} , where a is the scale factor of the universe. When the energy density drops to $\rho \sim N_{\text{IR}}^2 m_{\text{IR}}^4$, a confinement phase transition begins which lasts until the energy density has reached $\rho \sim g_s N_{\text{IR}} m_{\text{IR}}^4$ (see e.g. Appendix A in [11]; the phase transition in the dual gravity picture was studied in [12] using a 5d picture and in [13] using the full KS geometry). In the transition region for ρ , space is divided into separate regions in either the confined phase with $\rho < g_s N_{\text{IR}} m_{\text{IR}}^4$ or the (still) deconfined phase with $\rho > N_{\text{IR}}^2 m_{\text{IR}}^4$. At even lower energy densities $\rho < m_{\text{IR}}^4$ (assuming $g_s N_{\text{IR}} > 1$), a description in terms of a nonrelativistic glueball gas is applicable and the energy density

correspondingly scales with a^{-3} . We do not know the scaling of ρ with a in the transition region $N_{\text{IR}}^2 m_{\text{IR}}^4 > \rho > m_{\text{IR}}^4$ though, since the equation of state during the phase transition is unknown. Since we expect the scaling to be in between the two extremes $\rho \propto a^{-3}$ and $\rho \propto a^{-4}$ in this region, we will take $\rho \propto a^{-4}$ for $\rho > N_{\text{IR}} m_{\text{IR}}^4$ and $\rho \propto a^{-3}$ for $\rho < N_{\text{IR}} m_{\text{IR}}^4$ for simplicity.³

Let us first consider the case that the energy density deposited in a throat, Eq. (6), is larger than $\rho \sim N_{\text{IR}} m_{\text{IR}}^4$. If the gauge theory state created at reheating decays into a large number of glueballs with mass and kinetic energy of the order of m_{IR} , the gauge theory thermalizes. To see this in more detail, we view each initially created glueball as a localized excitation of a strongly coupled system with energy $\sim T_{\text{RH}}$. The localization assumption can be justified by recalling that, from the D-brane perspective, the mediating bulk supergravity fields couple to local gauge theory operators like $F_{\mu\nu} F^{\mu\nu}$. We model the further evolution of this state as a ball of gauge theory plasma expanding with the velocity of light.⁴ The number density of these balls is

$$n \sim \frac{\rho}{T_{\text{RH}}} \sim g^{1/2} N_{\text{UV}}^2 \frac{T_{\text{RH}}^6}{M_4^3}, \quad (9)$$

where we have used Eq. (6). It follows that the balls fill out the whole space after a time

$$t \sim n^{-1/3} \sim \frac{M_4}{g^{1/6} N_{\text{UV}}^{2/3} T_{\text{RH}}^2}. \quad (10)$$

Comparing this with the Hubble time Eq. (5) at $T = T_{\text{RH}}$, we see the gauge theory plasma fills out the whole space before the Hubble expansion becomes relevant if $N_{\text{UV}}^2 \gtrsim g$, which holds for all relevant throats.

The question of thermalization is more subtle if the gauge theory state produced at reheating decays into an $\mathcal{O}(1)$ number of the lightest glueballs with kinetic energies of the order of T_{RH} . We defer the corresponding discussion to Sect. 2.3. It turns out that in the cases of interest the glueballs again thermalize if the initial energy density is larger than $\rho \sim N_{\text{IR}} m_{\text{IR}}^4$. Furthermore, the initial decay vertex is strong enough to ensure that the potential energy $\sim m$ is transformed to the kinetic energy of the decay products instantaneously on the Hubble time scale.

Thus, we have found that in both extreme cases the energy density in the throat initially scales like radiation if it is above the phase transition density. It is given by

$$\rho \sim g^{1/2} N_{\text{UV}}^2 \left(\frac{T_{\text{RH}}}{M_4} \right)^3 T^4, \quad (11)$$

where T is the standard model temperature. We assume the scaling behaviour to change

³ Using the intermediate value $\rho \sim N_{\text{IR}} m_{\text{IR}}^4$ for the distinction between the two behaviours, the error in ρ is a factor of $(N_{\text{IR}} m_{\text{IR}}^4 / N_{\text{IR}}^2 m_{\text{IR}}^4)^{1/4} = N_{\text{IR}}^{-1/4}$ if $\rho \propto a^{-3}$ in the entire transition region or a factor of $(N_{\text{IR}} m_{\text{IR}}^4 / m_{\text{IR}}^4)^{1/3} = N_{\text{IR}}^{1/3}$ if $\rho \propto a^{-4}$ in the entire transition region. In both cases, this factor is typically $\mathcal{O}(1)$.

⁴ Note that this physical picture is equivalent to the picture of a cascade decay used in the derivation of Eq. (4) if we assume that a glueball with mass $m/2^n$ fills out a volume $(2^n/m)^3$.

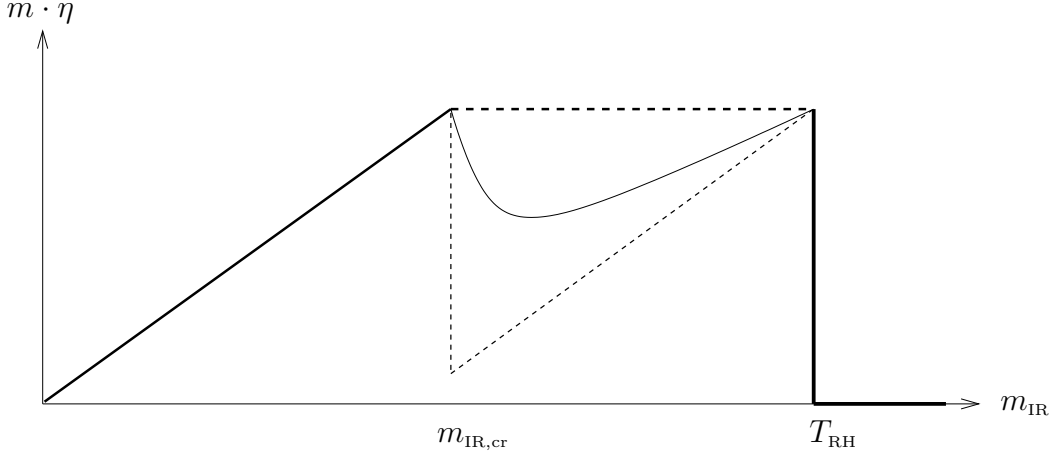


Figure 1: Schematic plot of $m \cdot \eta$ as a function of the IR scale m_{IR} of the throat. Here, $m_{\text{IR,cr}}$ is the IR scale for which $T_{\text{pt}} \sim T_{\text{RH}}$, i.e., for which the throat is heated precisely to its phase transition temperature. See text for more details.

when the energy density has dropped to $\rho \sim N_{\text{IR}} m_{\text{IR}}^4$. This happens when the standard model has a temperature

$$T_{\text{pt}} \sim m_{\text{IR}} \frac{N_{\text{IR}}^{1/4}}{N_{\text{UV}}^{1/2}} \left(\frac{M_4}{T_{\text{RH}}} \right)^{3/4}, \quad (12)$$

where we have neglected a factor of $g^{1/8}$ which is close to 1. The energy density scales like matter afterwards and the ratio of energy density and entropy density, $\rho/s = m \cdot \eta$, stays constant. Here $\eta = n/s$ is the glueball number density normalized by the entropy density. Using Eq. (11) and $s = g \frac{2\pi^2}{45} T^3$ (dominated by the standard model sector) at $T = T_{\text{pt}}$, we find the glueball mass density per entropy density

$$m \cdot \eta \sim \frac{N_{\text{UV}}^2}{g^{1/2}} \left(\frac{T_{\text{RH}}}{M_4} \right)^3 T_{\text{pt}}. \quad (13)$$

The factor of T_{pt} is smaller than or equal to T_{RH} and reflects the fact that the corresponding energy density undergoes a phase of a^{-4} dilution. The quantity $m \cdot \eta$ is useful because it determines the contribution of the glueballs to the total energy density in the late universe. We have plotted $m \cdot \eta$ as a function of m_{IR} schematically in Fig. 1. The part corresponding to Eq. (13) is the straight bold line which grows linearly⁵ with the IR scale from $m_{\text{IR}} = 0$ up to an m_{IR} such that T_{pt} in Eq. (12) is of the same order of magnitude as T_{RH} . This is the maximal IR scale for which Eq. (13) is valid because at this point the initial energy density in the throat, Eq. (6), is of the same order of magnitude as the critical energy density $\rho \sim N_{\text{IR}} m_{\text{IR}}^4$.

⁵ Note that this plot has to be read either at fixed N_{UV} , in which case N_{IR} must be interpreted as function of N_{UV} and m_{IR} , or at fixed N_{IR} , in which case N_{UV} must be interpreted as function of N_{IR} and m_{IR} . In both cases an extra logarithmic dependence of $m \cdot \eta$ on m_{IR} is introduced, which we however neglect.

Dividing Eq. (13) by $\rho_c/s_0 \simeq 2 \cdot 10^{-9}$ GeV, where ρ_c is the current critical energy density for a flat universe and s_0 is the current entropy density, and using $g \sim 100$ as well as $M_4 \simeq 2 \cdot 10^{18}$ GeV, we have

$$\Omega = \frac{\rho}{\rho_c} \sim \left(\frac{T_{\text{RH}} N_{\text{UV}}^{1/2}}{6 \cdot 10^{11} \text{ GeV}} \right)^4 \left(\frac{T_{\text{pt}}}{T_{\text{RH}}} \right). \quad (14)$$

This is the contribution of the throat sector to the density parameter. The second factor is smaller than or equal to 1 and again reflects the fact that the corresponding energy density undergoes a phase of a^{-4} dilution.

Let us now consider the case that the energy density deposited in a throat, Eq. (6), is smaller than $\rho \sim N_{\text{IR}} m_{\text{IR}}^4$. If the initial gauge theory state settles into a large number of slow glueballs, the energy density scales like matter from the beginning. Taking this scaling into account, the mass density over entropy density $m \cdot \eta$ is given by Eq. (13) with T_{pt} replaced by T_{RH} . Similarly, the contribution of the throat sector to the density parameter Ω is given by Eq. (14) with the second factor in brackets replaced by 1. As a function of m_{IR} , $m \cdot \eta$ is constant in this case, which we have plotted as the bold dashed line in Fig. 1.

The analysis is more subtle if the initial gauge theory state decays into an $\mathcal{O}(1)$ number of fast glueballs. The important question is again whether the glueballs thermalize because this determines the distribution of kinetic energies directly after reheating. As we will see in Sect. 2.3, in the cases of interest the glueballs do not thermalize if the initial energy density is smaller than $\rho \sim N_{\text{IR}} m_{\text{IR}}^4$. Since the glueballs are thus ultrarelativistic initially with kinetic energies of the order of T_{RH} , the energy density scales like radiation until the glueballs become nonrelativistic. Taking this into account, the contribution of the throat sector to the total energy density is determined by Eqs. (13) and (14) with T_{pt} replaced by m_{IR} . We have plotted $m \cdot \eta$ as a function of m_{IR} for this case as the thin dashed line in Fig. 1.

Finally, throats with $m_{\text{IR}} > T_{\text{RH}}$ are not heated for kinematic reasons. Therefore, the mass density over entropy density $m \cdot \eta$ is zero in this region, which we have plotted as a bold straight line in Fig. 1. Now, the bold straight lines in Fig. 1 correspond to regions where the function is the same in both extremal cases. We therefore expect that, in these regions, the plotted function gives the true behaviour also in intermediate cases (e.g. the decay of the initial gauge theory state into a large number of glueballs with a complicated distribution of kinetic energies). The thin dashed lines corresponds to the decay into a small number of highly-energetic glueballs whereas the bold dashed line corresponds to the decay into a large number of slow glueballs. We expect the true behaviour in this region to be in between these two extremes. We have plotted our expectation schematically as the thin curve.

2.3 Subtleties with thermalization

In this section, we consider the question of thermalization for the case that the initial gauge theory state decays into an $\mathcal{O}(1)$ number of highly-energetic glueballs. Let us

assume that this decay is fast⁶ compared to the Hubble time scale Eq. (5). The number density of the decay products is then given by Eq. (9) directly after reheating. If $n \langle \sigma v \rangle > H$, where $\langle \sigma v \rangle$ is the thermally averaged product of interaction cross section σ and velocity v , the glueballs thermalize. Since the glueballs have high energies $E \sim T_{\text{RH}} \gg m_{\text{IR}}$, their velocity v is close to 1. For energies

$$E \gg N_{\text{IR}}^2 m_{\text{IR}}, \quad (15)$$

the scattering cross section of KK modes in a throat or, equivalently, of glueballs in the dual gauge theory fulfills the Froissart bound and is given by [14]

$$\sigma \sim m_{\text{IR}}^{-2} \ln^2 \left(\frac{E}{m_{\text{IR}}} \right). \quad (16)$$

The glueball number density Eq. (9) scales as $n \propto a^{-3}$. During radiation domination, $a \propto T^{-1}$. Therefore, $n \propto T^3$ as a function of the standard model temperature T . Since the Hubble rate Eq. (5) only scales as $H \propto T^2$, the criterion for thermalization⁷ is easiest to fulfill directly after reheating at $T \sim T_{\text{RH}}$. Neglecting the logarithm in Eq. (16), we find

$$m_{\text{IR}} \lesssim N_{\text{UV}} \frac{T_{\text{RH}}^2}{M_4} \quad (17)$$

as a criterion for thermalization of a given throat sector with IR scale m_{IR} .

In Sect. 2.2, we have assumed that the glueballs thermalize if and only if the initial energy density in the throat, Eq. (6), is smaller than or of the same order of magnitude as the critical energy density $\rho \sim N_{\text{IR}} m_{\text{IR}}^4$. Using Eq. (6), this criterion can be written as

$$m_{\text{IR}} \lesssim \left(g^{-1/2} N_{\text{IR}} N_{\text{UV}}^2 \frac{T_{\text{RH}}}{M_4} \right)^{-1/4} N_{\text{UV}} \frac{T_{\text{RH}}^2}{M_4}. \quad (18)$$

As we will discuss in Sect. 4.1, N_{UV} can vary in the range $10 \lesssim N_{\text{UV}} \lesssim 10^4$. It then follows from Eq. (14) that the reheating temperature has to be between 10^{10} GeV and 10^{11} GeV if throat dark matter is not to be negligible today. Given the numerically large prefactor $g^{-1/2} N_{\text{IR}} N_{\text{UV}}^2$ in Eq. (18) and the exponent 1/4, it turns out that the criteria in Eqs. (17) and (18) are roughly equivalent. This justifies our previous simplifying assumption that a throat thermalizes if and only if the energy deposited in it is higher than its critical energy density.

Finally, let us discuss throat sectors which thermalize according to Eq. (17) in more detail. The high-energy scattering cross section of KK modes in Eq. (16) is dominated by the production of black holes localized near the IR end of the throat [14]. In the

⁶ As already mentioned, the process corresponding to the primary vertex is always fast since we are dealing with a strongly coupled system. However, similarly to QCD processes with final state jets, the hadronization time scale may be much slower. Thus, strictly speaking, we should derive the thermalization criterion taking into account the evolution of the decay products into glueballs. Since we are only interested in order-of-magnitude estimates, we neglect these subtleties in the following.

⁷The dependence of $\langle \sigma v \rangle$ on T via the glueball energy E is only logarithmic in the energy range of interest according to Eq. (16).

gauge theory, these black holes correspond to so-called plasma-balls, localized lumps of gauge theory plasma above the critical temperature, which are classically stable [11]. We expect the thermalization to proceed as follows: Two glueballs incident with an impact parameter smaller than $\sqrt{\sigma}$ at high energy will produce a plasma-ball. Other glueballs will be absorbed by the plasma-ball [11] and different plasma-balls will merge into larger plasma-balls. If the energy density is large enough for the gauge theory to be in the deconfined phase, this process continues until the gauge theory plasma fills out the whole space. On the gravity side this corresponds to the growing of the black hole horizon until it completely replaces the IR end of the throat. Otherwise, if the energy density is such that the equilibrated gauge theory is in the confined phase, the plasma-balls hadronize again until the whole space is filled by a nonrelativistic glueball gas.

3 Relics in a throat

3.1 Processes in the hidden sector

After a confinement phase transition, glueballs with mass of the order of the confinement scale and with different spin are formed. Similarly, if the gauge theory does not thermalize, the initial gauge theory states created at reheating settle into a certain number of light glueballs. A number of papers [15–23] have calculated parts of the bosonic glueball spectrum of the KS gauge theory. In [21], masses of KK towers of 7 coupled scalar fields and the graviton polarized parallel to the uncompactified dimensions were determined. In particular, several scalar states lighter than the lowest spin-2 state were found. Their numerical technique, however, does not reveal to which linear combinations of the 7 scalar fields these masses belong. In [16], the mass of the lowest KK mode of the dilaton was calculated using some approximations in the geometry. Again, it was found to be lighter than a spin-1 and a spin-2 state [16, 17], but no other scalar states were calculated to compare with. In the light of these findings, we expect the lightest state in the bosonic sector to be a scalar glueball. We do not know, however, to which field fluctuations on the gravity side of the duality this glueball corresponds.

The KS gauge theory has $\mathcal{N} = 1$ supersymmetry and the lightest scalar glueball has a spin- $\frac{1}{2}$ superpartner. In a phenomenologically viable setup, supersymmetry is broken and the masses of the scalar and the spin- $\frac{1}{2}$ glueball are no longer degenerate. We have not completely settled the important question of the size of the mass splitting and which of the two superpartners is lighter. In the following, we will mainly be interested in scenarios with high-scale SUSY breaking. As we discuss in Sect. 5, we expect that the spin- $\frac{1}{2}$ glueball is lighter than its scalar superpartner in this case. Nevertheless, we keep the discussion as general as possible and allow for the two possibilities that the fermion is lighter or heavier than the scalar.⁸

⁸ It may happen that the lightest fermionic glueball is not the superpartner of the lightest bosonic glueball. The following discussion then stays correct if one replaces the spin- $\frac{1}{2}$ superpartner by this lightest fermionic glueball. Moreover, it may happen that the mass of the lightest bosonic glueball is larger than twice the mass of the lightest fermionic glueball. The former could then decay to the latter

Generically, the glueball effective theory includes various cubic interactions. For example, for a scalar glueball \mathcal{G} , a spin-1 glueball \mathcal{A}_μ and a spin-2 glueball $\mathcal{H}_{\mu\nu}$, there are couplings of the type

$$\partial_\mu \mathcal{G} \mathcal{A}_\nu \mathcal{H}^{\mu\nu} + m_{\text{IR}} \mathcal{A}_\mu \mathcal{A}^\mu \mathcal{G} + m_{\text{IR}}^{-1} \partial_\mu \mathcal{G} \partial_\nu \mathcal{G} \mathcal{H}^{\mu\nu} + \dots \quad (19)$$

The coupling strengths follow on dimensional grounds up to possible factors of N_{IR} that we have not determined. Also, there may be more partial derivatives involved or they may act differently. Due to interactions of this type, heavy glueballs decay quickly to a few light states which cannot decay further for kinematic reasons. Note, however, that the KS gauge theory has a global $\text{SU}(2) \times \text{SU}(2)$ symmetry which forbids certain couplings of the type of Eq. (19). From the dual gravity point of view, this symmetry corresponds to an isometry of the KS throat. In a compactified setup, the KS throat is attached to a Calabi-Yau manifold which breaks this isometry in the UV. This symmetry breaking is mediated to the IR as discussed in [24–26]. We therefore expect that couplings of the type of Eq. (19), which violate the global symmetry, are nevertheless present, albeit with a possibly smaller coupling strength. In the following, we ignore the effects of glueballs charged under the $\text{SU}(2) \times \text{SU}(2)$ symmetry. In particular, we expect that the lightest scalar glueball and its superpartner are singlets with respect to this symmetry.

If the gauge theory has thermalized, the glueballs which can not decay interact with each other for a certain period of time after the confinement phase transition. This leads to a significant reduction of the abundances of all the states heavier than the lightest glueball, including its superpartner if the mass splitting from supersymmetry breaking is not too small. We now analyse this effect in some detail:

For simplicity, we focus on only two glueball species. Generically, the glueball effective action includes couplings of the type

$$\mathcal{H}\mathcal{H}\mathcal{G}\mathcal{G}, \quad (20)$$

where \mathcal{H} and \mathcal{G} are the heavy and light glueball respectively, and all Lorentz- and/or spinor-indices are appropriately contracted. By assumption, the masses of the two glueball species satisfy $m_{\mathcal{G}} < m_{\mathcal{H}}$. As long as the two glueball species are in equilibrium, the density $n_{\mathcal{H}}$ of the heavy glueballs is suppressed relative to the light glueball density $n_{\mathcal{G}}$ by an exponential factor $\exp[-(m_{\mathcal{H}} - m_{\mathcal{G}})/\tilde{T}]$ after the temperature \tilde{T} of the glueball gas falls below m_{IR} . This exponential decrease of the number density of \mathcal{H} glueballs continues until they are so dilute that they decouple. This happens, when

$$n_{\mathcal{H}} \cdot \langle \sigma v \rangle \sim H. \quad (21)$$

Here $\langle \sigma v \rangle$ is the thermally averaged product of cross section and relative velocity for the $2 \cdot \mathcal{H} \leftrightarrow 2 \cdot \mathcal{G}$ process, which evaluates to [27]⁹

$$\langle \sigma v \rangle \sim m_{\text{IR}}^{-2}. \quad (22)$$

via couplings discussed below. We will not consider this possibility in the following.

⁹If the mass difference $m_{\mathcal{H}} - m_{\mathcal{G}}$ is very small, this cross-section is kinematically suppressed. This may happen, for example, for the superpartner of the lightest glueball. These glueballs are then diluted to a lesser extent.

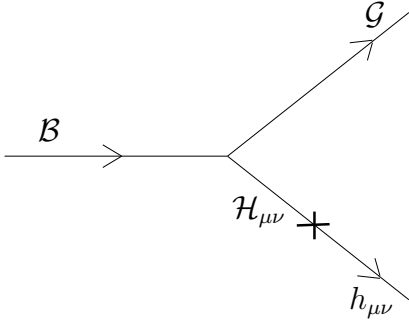


Figure 2: Decay of a bosonic glueball \mathcal{B} into a scalar glueball \mathcal{G} and a graviton $h_{\mu\nu}$ via a spin-2 glueball $\mathcal{H}_{\mu\nu}$.

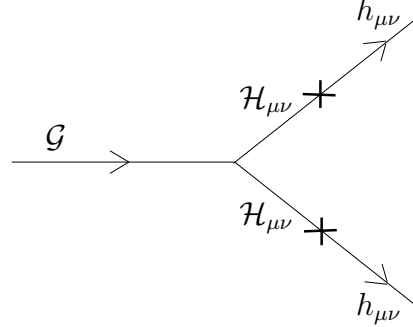


Figure 3: Decay of a scalar glueball \mathcal{G} into two gravitons $h_{\mu\nu}$ via spin-2 glueballs $\mathcal{H}_{\mu\nu}$.

Since $n_{\mathcal{H}}$ drops exponentially after the temperature \tilde{T} falls below m_{IR} , the heavy glueballs decouple when the temperature of the glueball gas is still of the same order of magnitude as the IR scale. We can therefore derive the freezeout density of the heavy glueballs from Eq. (21) using the phase-transition Hubble rate $H(T_{\text{pt}})$. Furthermore, we can approximate the light glueball density by m_{IR}^3 . The ratio of heavy and light glueball densities directly after freezeout, i.e. the dilution factor, is then given by

$$\frac{n_{\mathcal{H}}}{n_{\mathcal{G}}} \sim \frac{H(T_{\text{pt}})}{m_{\text{IR}}} \sim \frac{g^{1/2} m_{\text{IR}} M_4^{1/2}}{N_{\text{UV}} T_{\text{RH}}^{3/2}}. \quad (23)$$

Here we have calculated the Hubble rate according to Eqs. (5) and (12) and disregarded a small power of N_{IR} . Our formula is valid if the right-hand side is smaller than 1. If, however, the right-hand side is formally larger than 1, the \mathcal{H} glueballs are decoupled from the beginning and not diluted at all.

At a later time, all bosonic glueballs which are left over from this process decay by emission of a graviton into the lightest scalar glueball. Namely, as we will discuss in Sect. 3.2, spin-2 glueballs mix with the 4d graviton. The corresponding vertex will be derived in Sect. 3.2 and is given in Eq. (27). Combined with interactions of the type given in Eq. (19), processes such as that shown in Fig. 2 are possible: A bosonic glueball \mathcal{B} decays to the lightest scalar glueball \mathcal{G} and, via a virtual spin-2 glueball $\mathcal{H}_{\mu\nu}$, to the graviton $h_{\mu\nu}$. Since the mixing between graviton and spin-2 glueball is $\sim N_{\text{UV}}/M_4$ (see Eq. (27)) and m_{IR} is the only other relevant dimensionful parameter, we have

$$\Gamma \sim N_{\text{UV}}^2 \frac{m_{\text{IR}}^3}{M_4^2} \quad (24)$$

for the corresponding decay rate (up to an unknown factor related to N_{IR} which may result from the three-globall vertex). Similarly, fermionic glueballs decay to the lightest spin- $\frac{1}{2}$ glueball and a graviton. The corresponding decay rate is again given by Eq. (24). In addition, fermionic glueballs may in principle decay to lighter bosonic glueballs and vice versa by emission of a gravitino. Indeed, by supersymmetry we expect a mixing of

spin- $\frac{3}{2}$ glueballs with the gravitino, again with the vertex given in Eq. (27). This would allow for the corresponding processes. As we have mentioned at the beginning of this section, we mainly focus on a setup in which the gravitino is very heavy and such decays are kinematically forbidden. In this case, a non-negligible amount of the superpartner of the lightest glueball is left.

At an even later time, the lightest scalar glueballs decay into two gravitons. Indeed, using the three-glueball coupling and the vertex in Eq. (27), the process shown in Fig. 3 is possible. The corresponding decay rate is

$$\Gamma \sim N_{\text{UV}}^4 \frac{m_{\text{IR}}^5}{M_4^4} \quad (25)$$

up to an unknown factor depending on N_{IR} . By supersymmetry, we expect that the lightest spin- $\frac{1}{2}$ glueballs may decay to a graviton and a gravitino with the same rate. As before, if the gravitino is very heavy, such decays are kinematically forbidden.

3.2 Decay to the standard model sector

Of the processes described so far, only the decay to two gravitons (or to graviton and gravitino, if the gravitino is light enough) can be sufficiently slow to be relevant for late cosmology. The other processes have a time scale much shorter than the age of the universe for all relevant choices of parameters. Thus, in late cosmology, the energy density in the throat sector is completely in the form of the lightest glueball and its superpartner. The abundance of the heavier superpartner is depleted by the factor in Eq. (23) if the gauge theory was thermalized.

The glueballs couple (very weakly) to the standard model and other throats. Therefore, they may decay to these sectors. In [7], we have calculated the decay rate of a dilaton between two $\text{AdS}_5 \times S^5$ throats embedded in a 6d torus. Again, we chose the dual picture where the throats are replaced by corresponding brane stacks. The calculation is then almost identical to the calculation of the energy transfer rate described at the beginning of Sect. 2. A crucial difference is the fact that the coupling between the glueball on a brane stack (corresponding to the dilaton in the throat) and the dilaton in the embedding torus cannot be read off from any Lagrangian since the glueball is a non-perturbative object. Therefore, in [7], we first used the gravity picture to calculate the decay rate for the following simplified setup: We considered a single finite throat embedded in flat 10d space and a dilaton KK mode decaying from the throat to the asymptotically flat region. Then, we determined the glueball-dilaton vertex from the requirement that the decay rate be reproduced in the gauge theory picture. Let us restrict ourselves to a glueball corresponding to an s-wave of the dilaton with respect to the S^5 in the throat. The vertex between the dilaton in the embedding torus and such a glueball on a brane stack is then given by (cf. Eq. (37) of [7])

$$N_{\text{UV}} \frac{m_{\text{IR}}^{1/2} m^{5/2}}{M_{10}^4}, \quad (26)$$

where m is the mass of the glueball (for our purposes $m \sim m_{\text{IR}}$). Note that Eq. (26) gives the vertex in the 10d effective theory. Thus, to be part of a Lagrangian, this vertex has to be multiplied by a 6d δ -function for the brane stack, the 4d glueball field of mass dimension 1 and the 10d dilaton field of mass dimension 4. As we have outlined in [7], Eq. (26) also works for a KS throat as long as the field corresponding to the glueball satisfies the equations of motion of a massless 5d scalar.

A simple example is provided by the 10d graviton $\hat{h}_{\mu\nu}$ polarized parallel to the uncompactified dimensions which fulfills the equation of motion of a massless, minimally coupled 10d scalar field [18,28]. It also obeys the equations of motion of a massless scalar in the 5d effective theory of the throat. The vertex between the corresponding glueballs and $\hat{h}_{\mu\nu}$ in the embedding manifold is again given by Eq. (26). We want to calculate the decay rate of such glueballs to another brane stack on which the standard model may live or which may correspond to another throat. This decay is mediated by the tower of KK modes of $\hat{h}_{\mu\nu}$ in the embedding manifold. In analogy to the energy transfer rate of Sect. 2, the contribution of the zero mode in this KK expansion dominates if the distance A between the two brane stacks is of the same order of magnitude as the size L of the embedding manifold.¹⁰ Normalizing this zero mode contributes an extra factor of L^{-3} to the vertex of Eq. (26). Using $M_4 \simeq M_{10}^4 L^3$, the vertex of the 4d effective theory characterizing the mixing of the spin-2 glueball and the 4d graviton is thus given by

$$N_{\text{UV}} \frac{m_{\text{IR}}^{1/2} m^{5/2}}{M_4}. \quad (27)$$

This is similar to the mixing between the photon and the ρ meson known from QCD and was also observed in [29] for the gauge theory dual of a 5d RS model. Using Eq. (27) and the fact that the 4d graviton couples to the energy-momentum tensor on the other brane stack with strength M_4^{-1} as well as summing over all degrees of freedom on the other brane stack, we get

$$\Gamma \sim N^2 N_{\text{UV}}^2 \frac{m^4 m_{\text{IR}}}{M_4^4}. \quad (28)$$

This is the decay rate of a spin-2 glueball (which is a singlet with respect to the R-symmetry of the gauge theory) to another brane stack.

The vertex Eq. (27) also applies to the coupling of scalar glueballs to zero modes of other fields in the embedding manifold. To see this, let us consider the dilaton ϕ , whose equation of motion is

$$\nabla^2 \phi = \frac{1}{12} e^\phi \tilde{F}_{MNP} \tilde{F}^{MNP} - \frac{1}{12} e^{-\phi} H_{MNP} H^{MNP}. \quad (29)$$

Here, $\tilde{F}_3 = F_3 - CH_3$ and $F_3 = dC_2$ and $H_3 = dB_2$ are the field strengths of the Ramond-Ramond 2-form C_2 and the Neveu-Schwarz 2-form B_2 , respectively. Moreover, C is the Ramond-Ramond scalar, which we have taken to be constant in Eq. (29). In a background with imaginary self-dual 3-form flux [10], the flux fulfills

$$H_{MNP} H^{MNP} = e^{2\phi} \tilde{F}_{MNP} \tilde{F}^{MNP} \quad (30)$$

¹⁰ More generally, there is again a term with an A^{-8} dependence in the expression for the decay rate. This term becomes dominant at small A , see [7].

for the background value of ϕ and the right-hand side of Eq. (29) vanishes. This is no longer the case if one shifts the background value of ϕ while keeping B_2 and C_2 fixed. However, if one simultaneously shifts B_2 in such a way that Eq. (30) remains fulfilled, the right-hand side of Eq. (29) still vanishes. In other words, there exists a flat direction in the 5d effective theory which one can parameterize, e.g., by the value of the dilaton. The corresponding field then fulfills the equation of motion of a 5d minimally coupled, massless scalar. A light glueball, i.e. a KK mode localized at the bottom of the throat, will generically mix with this flat direction in the upper part of the throat [30,31]. Thus, scalar glueballs couple to zero modes in the embedding manifold with the previously derived vertex Eq. (27).

Note also that stronger couplings may arise for glueballs mixing with fields of the 5d effective theory which have tachyonic mass. The reason is that the 5d profile of such fields is suppressed more weakly if one moves from the IR to the UV end of the approximate AdS₅ geometry. It may be worthwhile to investigate this effect in more detail in the future.

A crucial difference to the decay of spin-2 glueballs is the fact that the mediating field is massive if fluxes are present in the compact space containing the two brane stacks [10]. More specifically, the zero mode of the (axion-)dilaton and the complex structure moduli get a mass

$$m_\tau \sim \frac{M_{10}^2}{M_4}, \quad (31)$$

where we have assumed that $g_s \sim 1$. The Kähler moduli can be lighter. We discuss the possible effects of Kähler moduli in mediating decays in Sect. 5.

Redoing the calculation leading to Eq. (28) with a massive instead of a massless propagator for the mediating field, we get an extra factor of

$$\left(\frac{m^2}{m^2 - m_\tau^2}\right)^2 \sim \left(\frac{m}{m_\tau}\right)^4 \quad (32)$$

for the decay rate of a scalar glueball. In the last step, we have assumed that the dilaton (or the complex structure modulus) is heavier than the decaying glueball. In this case, Eq. (32) suppresses the decay rate.¹¹ Combining Eqs. (28) and (32) and using Eq. (31), we then get

$$\Gamma \sim N^2 N_{\text{UV}}^2 \frac{m^8 m_{\text{IR}}}{M_{10}^8} \quad (33)$$

for the decay rate of a scalar glueball to another brane stack. In particular, for $N^2 = g$, Eq. (33) is the decay rate of scalar glueballs to the standard model.

We have not yet determined the decay rate of the spin- $\frac{1}{2}$ glueballs. For unbroken supersymmetry, this rate is related to the scalar decay rate by a supersymmetry transformation and both rates are thus equal. We expect that even for broken supersymmetry, the relevant vertices agree up to $\mathcal{O}(1)$ prefactors and that the suppression of the spin- $\frac{1}{2}$

¹¹ One can check that the contribution of higher KK modes is still smaller than the zero mode contribution for m_τ given in Eq. (31).

decay rate by the dilatino propagator is the same as the suppression of the scalar decay rate by the dilaton propagator. Therefore, we can use Eq. (33) also for the decay rate of spin- $\frac{1}{2}$ glueballs to other throats.

The situation is more complicated for decays to the standard model. Namely, we have assumed that the gravitino is much heavier than the glueballs and, accordingly, that supersymmetry is broken at a high scale. This means that also the superpartners of standard model particles are heavier than the decaying spin- $\frac{1}{2}$ glueballs. If R-parity is conserved, most decay channels involve such a superpartner as a final state and the corresponding decays are therefore kinematically forbidden. A coupling that does not involve a superpartner is

$$\lambda \bar{l} \psi H, \quad (34)$$

where l is a lepton doublet, H is the Higgs doublet and ψ is a dilatino or any other modulino.¹² The coupling strength λ may be $\mathcal{O}(1)$ or it may be suppressed as $\lambda = m/M_4$ where m is some low mass scale. The coupling in Eq. (34) probably requires R-parity violation. Namely, the corresponding coupling containing the modulus instead of the modulino generates a bilinear R-parity violating term for nonzero modulus vev. But since we assume high-scale supersymmetry breaking, a large coupling λ may still be allowed. Moreover, even for maximally broken R-parity, all other decay channels involve standard model superpartners which further decay into standard model particles. The corresponding decay rates are therefore suppressed by the propagators of the heavy superpartners and are smaller than the decay rate resulting from Eq. (34). Therefore, we concentrate on this coupling in the following. Redoing the steps leading to Eq. (33) with the vertex of Eq. (34), we find

$$\Gamma \sim \lambda^2 N_{\text{uv}}^2 \frac{m^6 m_{\text{IR}}}{M_{10}^8 / M_4^2} \quad (35)$$

for the decay rate of spin- $\frac{1}{2}$ glueballs to the standard model. If the coupling in Eq. (34) is absent and R-parity is exactly conserved, the spin- $\frac{1}{2}$ glueballs can not decay at all to the standard model sector. If, in addition, there is no throat with lower IR scale (otherwise decays to this sector with the rate in Eq. (33) are possible), the spin- $\frac{1}{2}$ glueballs are absolutely stable.

Finally, the gravitino may also play a role in mediating decays of fermionic glueballs. We will discuss these effects in Sect. 5.

4 Cosmological scenarios

If the glueballs from a given throat are stable until our epoch, then these glueballs are an interesting dark matter candidate. We begin our discussion in Sect. 4.1 with scenarios where a single throat accounts for the observed dark matter. Essentially, this gives a relation for the required reheating temperature as a function of the IR scale of the

¹²This coupling was already considered in [32] since it also leads to a mixing between the modulino and the neutrino.

throat. In Sect. 4.2 we discuss the probably more natural scenario that various throats of different lengths are present. As we show, in this case a reheating temperature of $10^{10} - 10^{11}$ GeV naturally leads to the right dark matter abundance.

4.1 A single throat

We consider a setup in which the compact manifold contains a single throat. In order to evaluate the relevant equations from Sects. 2 and 3, we have to fix N_{IR} and N_{UV} . These numbers determine the warp factor $h = \exp(2\pi N_{\text{UV}}/3N_{\text{IR}})$ which in turn is related to the IR scale $m_{\text{IR}} \sim h^{-1}N_{\text{IR}}^{-1/4}M_{10}$ of the throat. To simplify the discussion and to avoid uncertainties associated with unknown factors of N_{IR} in the various glueball decay rates, we focus on throats where $N_{\text{IR}} = \mathcal{O}(1)$. N_{UV} is then a function of m_{IR} and M_{10} . For our purposes it will be sufficient to use the typical values $N_{\text{UV}} \sim 10$ for long throats (e.g. for $m_{\text{IR}} \sim 10^6$ GeV and $M_{10} \sim 10^{15}$ GeV) and $N_{\text{UV}} \sim 4$ for shorter throats (e.g. for $m_{\text{IR}} \sim 10^{11}$ GeV).

As we have explained in Sect. 2.2 and as one can see from Fig. 1, we expect the glueball mass density over entropy density $m \cdot \eta$ or, equivalently, the contribution of glueballs to the density parameter Ω to be maximized for throats with $m_{\text{IR}} \sim m_{\text{IR,cr}}$ and with $m_{\text{IR}} \sim T_{\text{RH}}$. Let us focus on throats with the former IR scale first. This IR scale is defined by the condition that the initial energy density in the throat, Eq. (6), is just the critical energy density $\rho \sim N_{\text{IR}}m_{\text{IR}}^4$ of that throat. Solving for m_{IR} , we have

$$m_{\text{IR,cr}} \sim \left(\frac{N_{\text{UV}}^2 T_{\text{RH}}^7}{N_{\text{IR}} M_4^3} \right)^{1/4}, \quad (36)$$

where we have neglected a factor of $g^{1/8}$ which is $\mathcal{O}(1)$. It follows from Eq. (12) that $T_{\text{pt}} \sim T_{\text{RH}}$ for this IR scale. Using $N_{\text{UV}} \sim 10$ and $T_{\text{pt}} \sim T_{\text{RH}}$ in Eq. (14), we see that a reheating temperature of the order of 10^{11} GeV leads to the right amount of dark matter. It follows from Eq. (36) that the mass of this dark matter candidate is

$$m_{\text{IR}} \sim 10^6 \text{ GeV}. \quad (37)$$

If the coupling in Eq. (34) is present, the spin- $\frac{1}{2}$ glueballs decay to the standard model with a rate given by Eq. (35). The resulting lifetime is

$$\tau \sim 10^{26} \left(\frac{M_{10} \cdot \lambda^{-1/4}}{2 \cdot 10^{16} \text{ GeV}} \right)^8 \text{ s}. \quad (38)$$

Note that we consider a setup in which the gravitino is heavier than the glueballs. The decay of spin- $\frac{1}{2}$ glueballs to a gravitino and a gravitino is therefore kinematically forbidden. It is not sufficient to make the lifetime in Eq. (38) just longer than the present age of the universe (which is $\sim 10^{17}$ s): The glueball decays produce photons (e.g. via hadronic showers) which contribute with a continuous spectrum to the diffuse γ -radiation. The γ -ray flux measured e.g. by the experiment EGRET gives constraints on the lifetime of

unstable particles in dependence of their mass density [33].¹³ In particular, an unstable particle with the mass density of dark matter has to live longer than $\sim 10^{26}$ s to comply with observations.¹⁴ Thus, it depends on the two unknown parameters M_{10} and λ whether the spin- $\frac{1}{2}$ glueballs are a good dark matter candidate or not.

An interesting scenario is a setup in which $\lambda = \mathcal{O}(1)$.¹⁵ To get a viable dark matter candidate, the 10d Planck scale has a rather limited range in this case according to Eq. (38). This makes it more probable that the lifetime of the glueballs is in a range that can be probed by more sensitive γ -ray telescopes like the upcoming satellite GLAST. If this scenario with $\lambda = \mathcal{O}(1)$ is realized in nature, one may be able to see a signal in the near future.

The scalar glueballs from a throat with IR scale 10^6 GeV decay to two gravitons after 10^{15} s. Note, however, that this lifetime is proportional to m_{IR}^{-5} (cf. Eq. (25)). The lifetime will thus be somewhat larger or smaller for IR scales slightly different from 10^6 GeV. If the lifetime is in the range of 10^{17} s (the present age of the universe) to 10^{12} s (the time of matter-radiation equality), the resulting decrease in the dark matter density may have interesting consequences for structure formation. As we will explain in Sect. 5, we expect the fermionic glueballs to be lighter than their scalar superpartners if the supersymmetry breaking scale is larger than the IR scale of the throat. Due to the mass difference, part of the scalar glueballs annihilate into their superpartners after the phase transition and the abundance of the scalar glueballs is depleted by the factor given in Eq. (23). Inserting the above values for N_{UV} , m_{IR} and T_{RH} in Eq. (23), we see that the scalar glueballs make up for only 10^{-2} of the total dark matter abundance and the loss of mass density by the decay of the scalar glueballs is correspondingly small. We can not exclude the possibility, however, that either the mass splitting due to supersymmetry breaking is very small or that the fermionic glueballs are heavier than a scalar superpartner. In these cases, the scalar glueballs are not diluted and the loss of dark matter mass density by the decay of the scalar glueballs is much larger. Namely, it drops by a factor of $\frac{1}{2}$ in the former case and by a factor of 10^{-2} in the latter case. It would be interesting to analyse these possibilities and their implications for cosmology in more detail. To this end, a better understanding of the effect of supersymmetry breaking on the glueball mass spectrum would be required.

If the lifetime of scalar glueballs is large enough, a non-negligible amount still exists at our epoch. Their decays to the standard model again produce γ -radiation. Using Eq. (33) with $m_{\text{IR}} \sim 10^6$ GeV, the partial lifetime of scalar glueballs for decays to the

¹³See e.g. [34–36] for other work on decaying dark matter.

¹⁴Here, we have used that the hadronic branching ratio for decays via the coupling in Eq. (34) is $\mathcal{O}(1)$. For decays exclusively to photons or leptons, the constraints are less severe.

¹⁵The coupling in Eq. (34) leads to a mixing between the modulino ψ and a (left-handed) neutrino ν after electroweak symmetry breaking. Since the modulino has a large mass m_τ , the seesaw mechanism results in a light mass eigenstate. For $M_{10} \sim 10^{16}$ GeV (the minimal value allowed for $\lambda \sim 1$ according to Eq. (38)), Eq. (31) gives $m_\tau \sim 10^{14}$ GeV. Using the mixing mass term for $\lambda \sim 1$ in the seesaw formula, the resulting neutrino mass is ~ 0.1 eV. Interestingly, this is precisely the mass range indicated by various experiments.

standard model is

$$\tau \sim 10^{26} \left(\frac{M_{10}}{3 \cdot 10^{13} \text{ GeV}} \right)^8 \text{ s.} \quad (39)$$

If the scalar glueballs (still) make up an $\mathcal{O}(1)$ fraction of the dark matter at our epoch, this partial lifetime has to be larger than $\sim 10^{26}$ s to comply with the EGRET measurements. If the current abundance of scalar glueballs is reduced (by decays to two gravitons or by annihilation if the fermionic superpartner is lighter), the lower bound on the lifetime becomes correspondingly weaker.

In contrast to fermionic glueballs, scalar glueballs can decay directly to two photons. Decays via this channel in the halo of our galaxy lead to a sharp γ -line in addition to the continuous spectrum. The γ -rays at energies around 10^6 GeV cannot be measured by EGRET or GLAST. Ground-based γ -ray telescopes like HESS have the necessary energy range, but a limited sensitivity due to the cosmic-ray background. At 10^6 GeV, the measured flux in the cosmic ray spectrum is (see e.g. [37])

$$F \sim 10^{-12} (\text{m}^2 \text{ sr s GeV})^{-1}. \quad (40)$$

To be detectable against this background, the flux from the decaying glueballs in the halo has to be of the same order of magnitude. This flux is emitted as a sharp line at energy $\sim m_{\text{IR}}$ but smeared out by the detector due to a finite energy resolution ΔE . We model this effect by replacing the δ -function peak of the flux by a box of width ΔE . The flux is also inversely proportional to the mass m_{IR} and the lifetime τ of the glueballs. Assuming that the scalar glueballs make up an $\mathcal{O}(1)$ fraction of the dark matter at our epoch, it is given by (see e.g. [35])

$$F \sim 10^{-12} \left(\frac{10^5 \text{ GeV}}{\Delta E} \right) \left(\frac{10^6 \text{ GeV}}{m_{\text{IR}}} \right) \left(\frac{10^{26} \text{ s}}{\tau} \right) (\text{m}^2 \text{ sr s GeV})^{-1}. \quad (41)$$

For $m_{\text{IR}} \sim 10^6$ GeV and $\Delta E \sim 10^{-1} \cdot E \sim 10^5$ GeV as quoted by the HESS collaboration, the partial lifetime of the scalar glueballs (for decays to the standard model) has to be less than $\sim 10^{26}$ s to be detectable against the cosmic ray background. If the partial lifetime is somewhat larger, the γ -line may nevertheless become detectable in the near future with an improved rejection of cosmic ray events and a better sensitivity and energy resolution.

Thus, if an $\mathcal{O}(1)$ fraction of the dark matter at our epoch are scalar glueballs and if their partial lifetime is not much larger than 10^{26} s, two experiments may see a signal: The contribution of glueball decays to the γ -ray spectrum below 10^2 GeV may be detected by GLAST. Furthermore, the γ -line near 10^6 GeV may be seen by HESS. A lifetime of the order of 10^{26} s follows if $M_{10} \sim 10^{13}$ GeV according to Eq. (39). Such a low 10d Planck scale may be realized in a large-volume compactification along the lines of [38]. Note that this scenario is incompatible with the aforementioned scenario in which $\lambda = \mathcal{O}(1)$: According to Eq. (38), λ has to be very small (or zero) for such a low 10d Planck scale.

We can also discuss throats with IR scales smaller than 10^6 GeV. As before, we take $N_{\text{UV}} \sim 10$. According to Eqs. (12) and (14), Ω is proportional to $T_{\text{RH}}^{9/4} m_{\text{IR}}$. In order still

to have the abundance of dark matter with $\Omega \sim 1$, we have to increase the reheating temperature as $T_{\text{RH}} \propto m_{\text{IR}}^{-4/9}$ if we lower the IR scale. For example, for a throat with IR scale 10^4 GeV, a reheating temperature of 10^{12} GeV would give the right abundance. Since the various glueball decay rates are proportional to m_{IR} to some positive power, the glueballs become more stable for lower IR scales.

Let us now consider throats with $m_{\text{IR}} \sim T_{\text{RH}}$ where $m \cdot \eta$ has another peak. We take $N_{\text{UV}} \sim 4$ in order to have $N_{\text{IR}} = \mathcal{O}(1)$. According to Eq. (14) for $T_{\text{pt}} \sim T_{\text{RH}}$, such a throat again gives the right amount of dark matter for a reheating temperature $\sim 10^{11}$ GeV. The mass of this dark matter candidate correspondingly is $\sim 10^{11}$ GeV. We expect that the glueballs are never in thermal equilibrium for such short throats. Therefore, the heavier superpartners do not annihilate into the lightest glueball states and the initial abundance of scalar and spin- $\frac{1}{2}$ glueballs is equal. The scalar glueballs decay to two gravitons already after 10^{-8} s, according to Eq. (25). If the coupling in Eq. (34) is present, the spin- $\frac{1}{2}$ glueballs decay to the standard model after

$$\tau \sim 10^{27} \left(\frac{M_{10} \cdot \lambda^{-1/4}}{5 \cdot 10^{20} \text{ GeV}} \right)^8 \text{ s.} \quad (42)$$

Hadronic decays of particles in this mass range have been considered in [39] to explain events in the cosmic ray spectrum beyond the GZK cutoff. Taking the measured flux in this energy range, claimed by several collaborations, as an upper limit, a lifetime of at least 10^{27} s is required for a particle with mass 10^{11} GeV. Thus, the spin- $\frac{1}{2}$ glueballs decay too quickly for $\lambda = \mathcal{O}(1)$ since M_{10} cannot be larger than $M_4 \simeq 2 \cdot 10^{18}$ GeV. The coupling λ can be much smaller, though, and the spin- $\frac{1}{2}$ glueballs may be sufficiently stable for large enough M_{10} .

Finally, we comment on throats with higher 5-form flux numbers N_{IR} and N_{UV} . Since N_{IR} is no longer of the order 1, we have only rough estimates of the glueball decay rates in these cases. In the following, we ignore this problem and assume that the glueballs are sufficiently stable. The number N_{UV} is constrained by the requirement that the Calabi-Yau has enough negative charge to compensate for the flux. If one considers the orientifold limit of an F-theory compactification, then this amount of negative charge is given by $\chi_4/24$, where χ_4 is the Euler number of the underlying Calabi-Yau four-fold. Examples with $\chi_4/24$ up to 10^4 are known (see e.g. [40]) and we thus have $N_{\text{UV}} \lesssim 10^4$. Let us consider throats with maximal $N_{\text{UV}} \sim 10^4$. It follows from Eq. (14) that throats at the two peaks $m_{\text{IR}} \sim m_{\text{IR,cr}}$ and $m_{\text{IR}} \sim T_{\text{RH}}$ of $m \cdot \eta$ can account for the dark matter if the reheating temperature was $\sim 10^{10}$ GeV. The mass of these dark matter candidates is $\sim 10^5$ GeV (using Eq. (36)) and $\sim 10^{10}$ GeV, respectively. Together with the results from the first part of this section (where we have chosen the other extreme with $N_{\text{IR}} = \mathcal{O}(1)$) this gives the possible range of parameters in our scenario if the 5-form flux number is varied from its minimal to its maximal value: The required reheating temperature is between 10^{10} GeV and 10^{11} GeV. Moreover, the IR scale can vary between 10^5 GeV and 10^6 GeV for a throat at the first peak of $m \cdot \eta$ or it is between 10^{10} GeV and 10^{11} GeV for a throat at the second peak.

4.2 Many throats

The distribution of vacua in the type IIB string theory landscape favours geometries with strongly warped regions or throats [3]. For the class of KKLT vacua [41], the statistical distribution of multi-throat configurations was estimated in [4]. It was found that the expected number of throats with a hierarchy h larger than some h_* for a given Calabi-Yau orientifold is

$$\bar{n}(h > h_* | K) = \frac{K}{3c \log h_*}, \quad (43)$$

where K is the number of 3-cycles of the Calabi-Yau and c is some unknown $\mathcal{O}(1)$ constant. Using the relation $m_{\text{IR}} \sim h^{-1} N_{\text{IR}}^{-1/4} M_{10}$ and neglecting the factor $N_{\text{IR}}^{-1/4}$ for simplicity, the expected number of throats with IR scale in the range $\hat{m}_{\text{IR}} < m_{\text{IR}} < \tilde{m}_{\text{IR}}$ follows from Eq. (43) and is given by

$$\bar{n}(\hat{m}_{\text{IR}} < m_{\text{IR}} < \tilde{m}_{\text{IR}} | K) = \frac{K/3c}{\log(M_{10}/\tilde{m}_{\text{IR}})} - \frac{K/3c}{\log(M_{10}/\hat{m}_{\text{IR}})}. \quad (44)$$

In the following, we evaluate Eq. (44) and the resulting dark matter scenarios for two specific cases, always assuming that $c = 1$. In the first case, we are optimistic about the number of 3-cycles, choosing $K = 200$. This is a moderately high but not untypical value within the set of known Calabi-Yau spaces [42]. It implies a larger number of throats, including throats with a relatively low IR scale. In this case, we focus on compactifications with a moderately large volume and a correspondingly low 10d Planck scale, $M_{10} \sim 10^{14}$ GeV. High values for M_{10} would lead to a long lifetime for the relatively light glueballs expected in this case. The observation of their decays would then be less likely.

In the second case, we are conservative by choosing $K \sim 60$. This number of 3-cycles is roughly the minimal value consistent with fine-tuning of the cosmological constant in the KKLT construction [4]. We expect only relatively short throats to be available in this case. Large-volume compactifications are then less interesting from a cosmological perspective since heavy glueballs will generically decay too quickly for low M_{10} . We thus focus on $M_{10} \sim 10^{18}$ GeV in the case $K = 60$.

Obviously, many other cases, including more extreme choices of parameters, are conceivable. However, an exhaustive study of the parameter space is beyond the scope of the present paper.

If many throats are present, we can expect that the observed dark matter (or at least the dominant throat contribution to dark matter) will come from throats with m_{IR} near one of the two maxima of $m \cdot \eta$ (cf. Fig. 1). As before, we will simplify the analysis by using $N_{\text{UV}} \sim 10$ for long throats ($m_{\text{IR}} \sim 10^6$ GeV) and $N_{\text{UV}} \sim 4$ for short throats ($m_{\text{IR}} \sim 10^{11}$ GeV). If dark matter is indeed due to such throats, the reheating temperature has to be $T_{\text{RH}} \sim 10^{11}$ GeV. Note that, in general, the situation might be more complicated: For example, a throat with an IR scale far away from the maxima but with very large N_{UV} (recall that N_{UV} is fairly arbitrary if we do not insist on $N_{\text{IR}} \sim 1$) may provide the dominant contribution to dark matter (cf. Eqs. (12) and (14)).

In the first example with $M_{10} \sim 10^{14}$ GeV, the lifetime of glueballs from a throat with $m_{\text{IR}} \sim 10^{11}$ GeV is much too short to be a good dark matter candidate (see below). Therefore, we focus on the maximum of $m \cdot \eta$ near $m_{\text{IR}} \sim 10^6$ GeV. The expected number of throats with this IR scale is

$$\bar{n} (5 \cdot 10^5 \text{ GeV} < m_{\text{IR}} < 5 \cdot 10^6 \text{ GeV}) \simeq 0.5. \quad (45)$$

Thus, a significant fraction of the vacua has a throat which yields the right amount of dark matter for $T_{\text{RH}} \sim 10^{11}$ GeV.¹⁶ Certain partial lifetimes of the glueballs have been discussed in Sect. 4.1. In addition, we now expect

$$\bar{n} (m_{\text{IR}} \lesssim 10^7 \text{ GeV}) \simeq 3.5 \quad (46)$$

throats with IR scales smaller than 10^6 GeV which provide another decay channel for the glueballs. These throats can have a large number G of degrees of freedom. Therefore, we have to check whether the lifetime of the dark matter glueballs is still larger than the current age of the universe. If we denote the 5-form flux number at the UV end of the i th throat by N_i , we have

$$G = \sum_i N_i^2, \quad (47)$$

where the sum runs over all throats with IR scales smaller than 10^6 GeV. Using Eq. (33) with $N^2 = G$, the partial lifetime of the glueballs for decays to these throats is

$$G^{-1} 10^{32} \text{ s}. \quad (48)$$

According to the discussion at the end of Sect. 4.1, we expect G to be somewhere in range of 10^2 to 10^8 . Thus, even for maximal G this partial lifetime is much larger than the current age of the universe and the glueballs are still a good dark matter candidate.

There are also throats with IR scales larger than 10^6 GeV. Since throats with IR scales larger than the reheating temperature are not heated for kinematic reasons, we are interested in throats between 10^7 GeV and 10^{11} GeV. Their average number is

$$\bar{n} (10^7 \text{ GeV} \lesssim m_{\text{IR}} \lesssim 10^{11} \text{ GeV}) \simeq 8.6. \quad (49)$$

Glueballs from these throats have shorter lifetimes than the dark matter glueballs. The abundance of particles which decay to the standard model with a lifetime between 10^{-2} s and 10^{12} s is severely constrained by nucleosynthesis [34, 43, 44]. Therefore, we have to check whether the decaying glueballs fulfill these bounds.¹⁷

We restrict ourselves to decays of scalar glueballs. The discussion can then be easily extended to include the fermionic glueballs. Since the fermionic glueballs decay to the

¹⁶ In deriving the energy transfer rates in Eqs. (1) and (2), we have assumed that the reheating temperature is smaller than the compactification scale, i.e. $T_{\text{RH}} < L^{-1}$. Using the relation $M_4 \sim L^3 M_{10}^4$, the compactification scale is $L^{-1} \sim 10^{12}$ GeV for a 10d Planck scale $M_{10} \sim 10^{14}$ GeV. Thus, the assumption is still fulfilled for such a low 10d Planck scale and a reheating temperature $T_{\text{RH}} \sim 10^{11}$ GeV.

¹⁷For lifetimes larger than 10^{12} s, bounds from the diffuse γ -radiation are important [33]. These are not relevant in this example.

standard model via the operator in Eq. (34), nucleosynthesis may give a bound on the coupling strength λ . Scalar glueballs have three important decay channels: They decay to two gravitons, to throats with lower IR scales and to the standard model. The total decay rate is the sum of the three corresponding decay rates. For a throat at 10^{11} GeV, the total decay rate is dominated by decays to throats with lower IR scales. Denoting by G the combined number of degrees of freedom of throats with $m_{\text{IR}} < 10^{11}$ GeV and using Eq. (28)¹⁸, the glueballs from such a throat decay already after $G^{-1}10^{-7}$ s. Since this lifetime is shorter than 10^{-2} s, these glueballs do not affect nucleosynthesis. Similarly, glueballs from a throat at 10^{10} GeV do not live long enough to be relevant for nucleosynthesis.

The lifetime becomes larger for throats with lower IR scales. We consider a throat at 10^7 GeV. The total decay rate is then dominated by decays to two gravitons since $G \lesssim 10^8$. Using Eq. (33), the corresponding lifetime is approximately 10^{10} s. Let us denote the mass density over entropy density of the fraction of glueballs that have decayed to the standard model sector by $m \cdot \eta_{\text{dec}}$. Successful nucleosynthesis requires that [44]

$$m \cdot \eta_{\text{dec}} \lesssim 10^{-14} \text{ GeV} \quad (50)$$

for particles that decay 10^{10} s after reheating.¹⁹ To estimate $m \cdot \eta_{\text{dec}}$, recall that $m \cdot \eta$ has maxima at IR scales $m_{\text{IR,cr}} \sim 10^6$ GeV and $T_{\text{RH}} \sim 10^{11}$ GeV (see Fig. 1). Calculating $m \cdot \eta$ at these IR scales from Eq. (13), we have

$$m \cdot \eta \lesssim 10^{-9} \text{ GeV}. \quad (51)$$

Using this upper value and taking the branching ratio for decays to the standard model sector into account, we get $m \cdot \eta_{\text{dec}} \lesssim 10^{-19}$ GeV for the fraction of scalar glueballs that may have affected nucleosynthesis. Thus, the bound in Eq. (50) is clearly fulfilled. Similarly, one can check that scalar glueballs from throats at 10^8 GeV and 10^9 GeV fulfill the bounds from nucleosynthesis. We conclude that glueball decays from throats between 10^7 GeV and 10^{11} GeV do not destroy nucleosynthesis.

In the second example, it is unlikely to find throats with $m_{\text{IR}} \sim 10^6$ GeV. Thus, we focus on the maximum of $m \cdot \eta$ near $m_{\text{IR}} \sim 10^{11}$ GeV. According to Eq. (44), the expected number of throats with IR scale between 10^{10} GeV and 10^{11} GeV is

$$\bar{n} (10^{10} \text{ GeV} \lesssim m_{\text{IR}} \lesssim 10^{11} \text{ GeV}) \simeq 0.3. \quad (52)$$

Thus, a significant fraction of the vacua has a throat in this range of IR scales. A reheating temperature of the order of 10^{11} GeV would give the right amount of dark matter not only for a throat at 10^{11} GeV but also for a throat at 10^{10} GeV: As one can see from

¹⁸ In deriving the decay rate in Eq. (33), we have assumed that the mass m_τ of the modulus which mediates the decay is larger than the mass m_{IR} of the decaying glueball. Using Eq. (31), we have $m_\tau \sim 10^{10}$ GeV for $M_{10} \sim 10^{14}$ GeV. For a throat with $m_{\text{IR}} \sim 10^{11}$ GeV, we therefore have to use the unsuppressed decay rate in Eq. (28).

¹⁹ The bounds on $m \cdot \eta_{\text{dec}}$ were derived for particles with masses in the range of 10^2 GeV to 10^4 GeV. At 10^{10} s, the bound is approximately independent of the particle mass. We therefore believe that it is a reasonable approximation to extrapolate this bound to particles of mass 10^7 GeV.

Fig. 1 (the thin curve), we expect the function $m \cdot \eta$ to decrease rather slowly with the IR scale near the peak at $m_{\text{IR}} \sim T_{\text{RH}}$. In the worst case, $m \cdot \eta$ is proportional to m_{IR} . From the discussion in Sect. 2.2, we also know that $m \cdot \eta$ is proportional to T_{RH}^3 . Thus, in order to compensate the decrease in $m \cdot \eta$ if m_{IR} is lowered by one order of magnitude, T_{RH} only has to be raised by an $\mathcal{O}(1)$ factor.

Certain partial lifetimes of the glueballs from such a throat have been discussed in Sect. 4.1. In addition, there may be throats with lower IR scales which provide new decay channels for the glueballs. Their expected number is

$$\bar{n} (m_{\text{IR}} \lesssim 10^9 \text{ GeV}) \simeq 1.1. \quad (53)$$

We denote the number of degrees of freedom of this sector by G . As before, we have to check that the dark matter glueballs do not decay too quickly to this sector. Using Eq. (33), the partial lifetime for this decay channel is

$$G^{-1} 10^{29} \text{ s} \quad \text{to} \quad G^{-1} 10^{20} \text{ s} \quad (54)$$

for glueball masses in the range of 10^{10} GeV to 10^{11} GeV. For large G , this lifetime is larger than the current age of the universe only for a throat around 10^{10} GeV. If G is small or if there is no throat with lower IR scale, also a throat around 10^{11} GeV would give a sufficiently stable dark matter candidate.

5 Further issues related to supersymmetry breaking

Up to now, we have neglected decays mediated by the Kähler moduli. This is justified if the Kähler moduli are sequestered from the throat sectors. The latter assumption follows from the interpretation of a Calabi-Yau orientifold with a long throat as supersymmetric Randall-Sundrum model in which the Kähler moduli are localized on the UV brane [45]. The sequestering assumption in this 5d framework [46] has been widely accepted and has also been used in the context of type-IIB models with strongly warped regions (see e.g. [47, 48] as well as the detailed discussion of [49] and refs. therein).

Let us restrict ourselves to the universal Kähler modulus. We denote the corresponding chiral superfield by T and a chiral glueball superfield from the throat sector by X . The Lagrangian can be written in standard $\mathcal{N} = 1$ supergravity form

$$\mathcal{L} = \int d^4\theta \varphi \bar{\varphi} \Omega + \left(\int d^2\theta \varphi^3 W + \text{h.c.} \right), \quad (55)$$

where $\varphi = 1 + \theta^2 F_\varphi$ is the chiral compensator, Ω is the kinetic function and W is the superpotential. The sequestering assumption [46] states that

$$\begin{aligned} \Omega(X, \bar{X}, T, \bar{T}) &= \Omega(X, \bar{X}) + \Omega(T, \bar{T}) \\ W(X, T) &= W(X) + W(T). \end{aligned} \quad (56)$$

In particular, terms mixing the superfields T and X appear neither in the kinetic part nor in the superpotential. Thus, since the universal Kähler modulus does not mix with

the glueballs, it cannot mediate their decays to other sectors. Even if the sequestered form of Eq. (56) turns out to be violated, we expect that the cross-couplings are much more suppressed than the mixing vertex of Eq. (26) between glueball and dilaton. The effect of the Kähler moduli in mediating glueball decays is then still negligible.

We have also not yet considered decays mediated by the gravitino. It may turn out that the fermionic glueball mixes with the gravitino which thus mediates its decay to other sectors. An additional process is the decay of the heavier superpartner to the lightest glueball by the emission of a gravitino. This follows from the process shown in Fig. 2 by replacing the virtual spin-2 glueball by a virtual spin- $\frac{3}{2}$ glueball, the outgoing graviton by a gravitino and one of the bosonic glueballs by a fermionic glueball. If the emitted gravitino is heavier than the decaying glueball, the gravitino is off-shell and must in turn decay to the standard model or another throat. It is not immediately clear, how strongly the propagator of the gravitino suppresses the corresponding decay rate, i.e. with which power the gravitino mass enters. In addition, the gravitino can be considerably lighter than the dilaton and complex-structure moduli. It may therefore turn out that we get a strong bound on the gravitino mass in our scenario. This would make it more probable that the decaying glueballs lead to a detectable signal. This is an interesting topic for future investigations.

Finally, let us consider the limit of light gravitinos or, equivalently, supersymmetry broken at a low scale. If the gravitino is lighter than the glueballs, the spin- $\frac{1}{2}$ glueballs may decay to a graviton and a gravitino as discussed at the end of Sect. 3.1. The scalar glueballs decay to two gravitons with the same rate. We have seen in Sect. 4.1 that the scalar glueballs with mass 10^6 GeV have a lifetime shorter than the current age of the universe. This lifetime would now also apply to the fermionic glueballs. But the partial lifetime for this decay channel is proportional to m_{IR}^{-5} according to Eq. (25). Thus, this problem does not occur if the infrared scale is somewhat lower than our ‘optimal’ value of 10^6 GeV. In this case, throat dark matter is still possible even if the SUSY breaking scale is low.

Many of the decay processes discussed in this and previous sections depend on the spectrum of the lightest glueballs from the throat sector. This spectrum depends crucially on the pattern of supersymmetry breaking in the throat, to which we now turn. Motivated by sequestering, we assume that supersymmetry breaking is communicated to the lightest glueball multiplet X only by the F-term F_φ of the chiral compensator.²⁰ The relevant part of the effective Lagrangian Eq. (56) is

$$\mathcal{L} \supset \int d^4\theta \varphi \bar{\varphi} X \bar{X} + \left(\int d^2\theta m X^2 \varphi^3 + \text{h.c.} \right). \quad (57)$$

If supersymmetry is broken, the F-term of the chiral compensator gets a vev $\langle F_\varphi \rangle$. Since we can expect this vev to be of the same order of magnitude as the gravitino mass, the

²⁰ Actually, the situation might be more complicated since the lightest glueball multiplet couples strongly to heavier glueballs, which are themselves affected by supersymmetry breaking and which might therefore influence the mass-splitting of the lightest multiplet in a non-negligible way. We intend to return to this point in future investigations and view the present calculation only as a reasonable first guess.

limit of a light gravitino corresponds to $\langle F_\varphi \rangle \ll m$. We can expand X in components and split the lowest component of X into real and imaginary parts. Inserting this expression in Eq. (57) and diagonalizing the resulting mass matrix for the real and imaginary part, one finds two scalar eigenstates with masses

$$m_{1,2}^2 = 4m^2 \pm 2m|\langle F_\varphi \rangle|. \quad (58)$$

Moreover, the mass of the fermion is $2m$ and receives no contribution from $\langle F_\varphi \rangle$. Therefore, one scalar glueball is lighter than its former spin- $\frac{1}{2}$ superpartner and the mass splitting is $|\langle F_\varphi \rangle|/2$. Depending on the precise relation between $\langle F_\varphi \rangle$ and the gravitino mass, the spin- $\frac{1}{2}$ glueball may or may not decay to the lighter scalar glueball by emission of a gravitino. If this decay is kinematically not allowed, the spin- $\frac{1}{2}$ glueball may still decay by mediation of a gravitino to standard model particles and the lighter scalar glueball. The gravitino propagator gives no suppression of the decay rate in this case and the decay rate is given by Eq. (28). For a throat with $m_{\text{IR}} \sim 10^6$ GeV and $N_{\text{IR}} \sim \mathcal{O}(1)$, the partial lifetime of the spin- $\frac{1}{2}$ glueballs for this decay channel is

$$\tau \sim 10^{15} \text{ s}. \quad (59)$$

Again, this is shorter than the current age of the universe. Since decays of this kind are constrained by diffuse γ -ray measurements, a partial lifetime larger than $\sim 10^{26}$ s is actually required. Since the partial lifetime is again proportional to m_{IR}^{-5} (cf. Eq. (28)), also this problem can be avoided with a lower IR scale. As we have explained in Sect. 4.1, this requires a higher reheating temperature.

Let us finally note that Eq. (58) is obviously not applicable if $\langle F_\varphi \rangle \gg m$. In this case, we can analyse the situation from the perspective of a chiral superfield with vanishing mass, i.e. we consider the limit $m \rightarrow 0$. The theory then possesses a chiral symmetry which ensures the masslessness of the fermion even in the presence of SUSY breaking. Thus, in analogy to the matter superfields of the minimal supersymmetric standard model, we expect that the scalar glueballs will be heavier than the fermions if supersymmetry breaking in the throat is a large effect relative to the supersymmetric mass term.

6 Summary

Strongly warped regions or throats are a common feature of the type IIB string theory landscape. KK modes whose wavefunctions are localized in a throat have redshifted masses, allowing for their production after reheating in the standard model sector, even if the reheating temperature is not very high. In addition, these KK modes are only very weakly coupled to the rest of the compact manifold, potentially resulting in a very long lifetime. These properties make the KK modes an interesting dark matter candidate.

We have considered a setup in which the standard model lives in the unwarped part of a compact manifold, which in addition has a certain number of throats. To be conservative, we have assumed that reheating only takes place in the standard model

sector. Even under this minimal assumption, the throats are heated up by energy transfer from the hot standard model plasma. In Sect. 2.1, we have determined the energy density deposited in a throat, using our result for the corresponding energy transfer rate from a previous paper [7].

Throats have a dual description as a strongly coupled gauge theory with a large number of colours. From this gauge theory point of view, the energy density in a throat is initially in the form of gauge theory states with energy of the order of the reheating temperature. These states subsequently settle into a certain number of lighter glueballs with some distribution of kinetic energies. The knowledge of this distribution is important since it determines whether the glueballs thermalize and whether (and for how long) the energy density scales like radiation or like matter. Since we are at present unable to determine this distribution of kinetic energies, we have considered two extremal cases in Sect. 2.2. In the first case, the initial gauge theory state settles into a large number of glueballs with kinetic energies of the order of their mass. In the second case, the decay products of the initial state are an $\mathcal{O}(1)$ number of glueballs which accordingly have kinetic energies of the order of the reheating temperature.

It turns out that the gauge theory thermalizes in both extremal cases if the energy density in this sector is above the critical energy density for deconfinement. The energy density thus scales like radiation under the expansion of the universe until the confinement phase transition takes place. Afterwards, it scales like matter. Taking this scaling into account, we have determined the contribution of the throat sector to the total energy density of the universe at our epoch. We have also determined this contribution for the case that the initial energy density in the throat sector is below the critical energy density and found that it differs considerably between the two extremal cases. We expect the true behaviour in this region of parameter space to be in between the two extremal cases.

After the confinement phase transition, different types of glueballs with mass of the order of the confinement scale m_{IR} are formed. Similarly, if the gauge theory does not thermalize, the initial gauge theory states created at reheating settle into a certain number of light glueballs. As we have shown in Sect. 3.1, these glueballs quickly decay to a lightest state and its superpartner. On the basis of a number of papers devoted to the spectrum of the KS gauge theory [15–23], we expect these lightest states to be a scalar glueball and its spin- $\frac{1}{2}$ superpartner. The glueballs couple (very weakly) to the standard model and other throats and can thus decay to these sectors. In Sect. 3.2, we have applied our results for this decay [7] to scalar glueballs. A crucial difference with respect to our previous analysis is the fact that the bulk fields which mediate the decay are massive in a flux background. Depending on the mass of the decaying glueballs, this can lead to a significant suppression of the corresponding decay rate. In addition, scalar glueballs can decay to two gravitons. We have determined the corresponding rate in Sect. 3.1.

Similarly, spin- $\frac{1}{2}$ glueballs can in principle decay to a graviton and a gravitino. To get a stable dark matter candidate, we are mainly interested in setups where such decays are kinematically forbidden due to a heavy gravitino. This requires that the supersymmetry breaking scale is larger than the mass of the glueball. It may also mean that the

superpartners of standard model particles are heavier than the glueballs. If R-parity is conserved, most decay channels of spin- $\frac{1}{2}$ glueballs to the standard model sector involve such a superpartner and are therefore kinematically forbidden. In Sect. 3.2, we have identified an operator which does not involve a superpartner and which would allow the decay of spin- $\frac{1}{2}$ glueballs to a Higgs and a lepton. If present, this operator would give the dominant decay channel even for maximally broken R-parity. Using the corresponding vertex, we have determined the decay rate of spin- $\frac{1}{2}$ glueballs to the standard model.

In Fig. 1, we have plotted the contribution of a throat sector to the total energy density of the universe for fixed reheating temperature T_{RH} and as a function of the IR scale m_{IR} . We expect this function to have two maxima at IR scales $m_{\text{IR,cr}}$ and T_{RH} . For a throat with IR scale $m_{\text{IR,cr}}$, the dual gauge theory thermalizes precisely to the phase transition temperature and therefore the energy density scales like matter immediately after reheating. KK modes in throats with IR scale T_{RH} , on the other hand, are so massive that they become nonrelativistic immediately after reheating and the energy density again scales like matter afterwards.

One of the main underlying ideas of our analysis is the generic presence of throats in the type IIB landscape. It is then probable to have throats with these optimal IR scales in a given compact manifold. For simplicity, we have first discussed a scenario with a single throat in Sect. 4.1. We have found that, in many cases, KK modes in throats with IR scale T_{RH} have a decay rate which is too high for them to be a good dark matter candidate. However, if the gravitino is very heavy (high-scale SUSY breaking) and certain operators connecting the standard-model and the moduli-sector are suppressed, the fermionic glueballs may nevertheless survive and play the role of dark matter.

The more promising case is that of throats with IR scale $m_{\text{IR,cr}}$, to which we now turn. In this case, it follows immediately from our results of Sect. 2.2 that a reheating temperature of 10^{10} GeV to 10^{11} GeV leads to the right amount of glueballs to account for the observed dark matter. The critical IR scale $m_{\text{IR,cr}}$ is a function of T_{RH} . After having fixed T_{RH} , we find a mass for our dark matter candidate which is between 10^5 GeV and 10^6 GeV. In Sect. 4.2, we have used results from Ref. [4] on the distribution of throats in the landscape to consider a scenario with a large number of throats. We have found that there are setups in which the probability of having a throat with the required IR scale is large. The only free parameter which has then to be fixed is the reheating temperature.

Our dark matter scenario may lead to some interesting observable signatures. The dark matter glueballs decay to the standard model with a very low, but non-negligible rate. The decays produce photons to which experiments like GLAST or HESS may be sensitive. It turns out that the decay rates depend on two parameters: The 10d Planck mass M_{10} enters via the flux stabilized mass of fields which mediate the decay. Moreover, the decay rate of spin- $\frac{1}{2}$ glueballs depends on the coupling strength λ of the aforementioned operator which allows their decay to a lepton and a Higgs. In Sect. 4.1, we have identified two interesting scenarios:

If λ is of the order 1, M_{10} has to be very large in order to get a sufficiently stable dark matter candidate. Namely, for a lower 10d Planck scale, the spin- $\frac{1}{2}$ glueballs decay to the standard model with a rate which is in conflict with measurements of the diffuse γ -

radiation. On the other hand, the 10d Planck scale cannot be larger than the 4d Planck scale. This makes it more probable that the lifetime of spin- $\frac{1}{2}$ glueballs is in a range that can be probed with new, more sensitive experiments like GLAST. If the scenario with $\lambda = \mathcal{O}(1)$ is realized in nature, one can hope to detect a signal from the decaying glueballs in the near future.

If λ is much smaller than 1, a lower M_{10} still leads to sufficiently stable spin- $\frac{1}{2}$ glueballs. For a low 10d Planck scale, also the decay of scalar glueballs can become relevant for detection. In contrast to fermionic glueballs, scalar glueballs can decay directly to two photons. This decay channel leads to a sharp γ -line at an energy of 10^5 GeV to 10^6 GeV which could be detected with experiments like HESS. In addition, the scalar glueball decays also produce a continuous γ -ray spectrum to which e.g. GLAST may again be sensitive. If the scalar glueballs make up an $\mathcal{O}(1)$ fraction of the dark matter at our epoch, a 10d Planck scale of the order of 10^{13} GeV would allow for a detection of both signals in the near future. Such a 10d Planck scale corresponds to a compactification radius of the order of just $50 l_{\text{string}}$, which is not extremely large.

Another interesting effect is the decay of the scalar glueballs into two gravitons which may happen before our epoch. Since we consider a setup in which the corresponding decay of the spin- $\frac{1}{2}$ glueballs into a graviton and a gravitino is kinematically forbidden, we still have a sufficiently stable dark matter candidate. For reasons that we have explained in Sect. 3.1, we expect the scalar glueballs to have a lower abundance than the spin- $\frac{1}{2}$ glueballs. The total dark matter abundance would then only change by a small factor when the scalar glueballs decay. It is possible, however, that the scalar glueballs have a comparable or even higher abundance than the spin- $\frac{1}{2}$ glueballs. The change in the dark matter abundance could then be enormous. It would be interesting to consider the implications of this scenario for cosmology.

In a setup with a large number of throats one also expects throats with IR scales larger than 10^5 GeV to 10^6 GeV (the IR scale of the throat which provides the dark matter). The glueballs from these throats have shorter lifetimes and may decay already during nucleosynthesis. Therefore, successful nucleosynthesis may impose further constraints on our scenario. For a particular example, we have checked in Sect. 4.2 that the glueball decays do not affect nucleosynthesis due to a low branching ratio to the standard model. Examples are conceivable, however, in which bounds from nucleosynthesis are only marginally fulfilled. It would then be interesting to look for traces of glueball decays in the abundances of light elements. Unfortunately, we are at present unable to determine the contribution of throats with the aforementioned range of IR scales to the total energy density of the universe with sufficient precision. Progress in this direction requires a detailed understanding of hadronization in a strongly coupled gauge theory, which we therefore view as a further interesting topic for future research.

Acknowledgements: We would like to thank F. Brümmer, W. Buchmüller, T. Dent, J. Ellis, W. Hofmann, K. Sigurdson and M. Trapletti for helpful discussions.

References

- [1] E. W. Kolb, D. Seckel and M. S. Turner, “The Shadow World,” *Nature* **314** (1985) 415;
J. R. Ellis, J. L. Lopez and D. V. Nanopoulos, “Confinement of fractional charges yields integer charged relics in string models,” *Phys. Lett. B* **247** (1990) 257;
A. E. Faraggi and M. Pospelov, “Self-interacting dark matter from the hidden heterotic-string sector,” *Astropart. Phys.* **16** (2002) 451 [arXiv:hep-ph/0008223];
J. A. R. Cembranos, A. Dobado and A. L. Maroto, “Brane-world dark matter,” *Phys. Rev. Lett.* **90** (2003) 241301 [arXiv:hep-ph/0302041];
G. Shiu and L. T. Wang, “D-matter,” *Phys. Rev. D* **69** (2004) 126007 [arXiv:hep-ph/0311228];
J. R. Ellis, V. E. Mayes and D. V. Nanopoulos, “Flipped cryptons and the UHE-CRs,” *Phys. Rev. D* **70** (2004) 075015 [arXiv:hep-ph/0403144].
- [2] S. Dimopoulos, S. Kachru, N. Kaloper, A. E. Lawrence and E. Silverstein, “Generating small numbers by tunneling in multi-throat compactifications,” *Int. J. Mod. Phys. A* **19** (2004) 2657 [arXiv:hep-th/0106128];
S. Dimopoulos, S. Kachru, N. Kaloper, A. E. Lawrence and E. Silverstein, “Small numbers from tunneling between brane throats,” *Phys. Rev. D* **64** (2001) 121702 [arXiv:hep-th/0104239].
- [3] F. Denef and M. R. Douglas, “Distributions of flux vacua,” *JHEP* **0405**, 072 (2004) [arXiv:hep-th/0404116];
A. Giryavets, S. Kachru and P. K. Tripathy, “On the taxonomy of flux vacua,” *JHEP* **0408** (2004) 002 [arXiv:hep-th/0404243];
J. P. Conlon and F. Quevedo, “On the explicit construction and statistics of Calabi-Yau flux vacua,” *JHEP* **0410** (2004) 039 [arXiv:hep-th/0409215];
T. Eguchi and Y. Tachikawa, “Distribution of flux vacua around singular points in Calabi-Yau moduli space,” *JHEP* **0601** (2006) 100 [arXiv:hep-th/0510061].
- [4] A. Hebecker and J. March-Russell, “The ubiquitous throat,” *Nucl. Phys. B* **781** (2007) 99 [arXiv:hep-th/0607120].
- [5] I. R. Klebanov and M. J. Strassler, “Supergravity and a confining gauge theory: Duality cascades and chiSB-resolution of naked singularities,” *JHEP* **0008** (2000) 052 [arXiv:hep-th/0007191].
- [6] X. Chen and S. H. Tye, “Heating in brane inflation and hidden dark matter,” *JCAP* **0606**, 011 (2006) [arXiv:hep-th/0602136].
- [7] B. v. Harling, A. Hebecker and T. Noguchi, “Energy Transfer between Throats from a 10d Perspective,” *JHEP* **0711** (2007) 042 [arXiv:0705.3648 [hep-th]].
- [8] A. Hebecker and J. March-Russell, “Randall-Sundrum II cosmology, AdS/CFT, and the bulk black hole,” *Nucl. Phys. B* **608** (2001) 375 [arXiv:hep-ph/0103214].

- [9] S. S. Gubser, “AdS/CFT and gravity,” *Phys. Rev. D* **63** (2001) 084017 [arXiv:hep-th/9912001];
D. Langlois, L. Sorbo and M. Rodriguez-Martinez, “Cosmology of a brane radiating gravitons into the extra dimension,” *Phys. Rev. Lett.* **89** (2002) 171301 [arXiv:hep-th/0206146];
D. Langlois and L. Sorbo, “Bulk gravitons from a cosmological brane,” *Phys. Rev. D* **68** (2003) 084006 [arXiv:hep-th/0306281].
- [10] S. B. Giddings, S. Kachru and J. Polchinski, “Hierarchies from fluxes in string compactifications,” *Phys. Rev. D* **66** (2002) 106006 [arXiv:hep-th/0105097].
- [11] O. Aharony, S. Minwalla and T. Wiseman, “Plasma-balls in large N gauge theories and localized black holes,” *Class. Quant. Grav.* **23** (2006) 2171 [arXiv:hep-th/0507219].
- [12] P. Creminelli, A. Nicolis and R. Rattazzi, “Holography and the electroweak phase transition,” *JHEP* **0203** (2002) 051 [arXiv:hep-th/0107141];
B. Hassanain, J. March-Russell and M. Schwelling, “Warped Deformed Throats have Faster (Electroweak) Phase Transitions,” arXiv:0708.2060 [hep-th].
- [13] O. Aharony, A. Buchel and P. Kerner, “The black hole in the throat - thermodynamics of strongly coupled cascading gauge theories,” arXiv:0706.1768 [hep-th];
M. Mahato, L. A. P. Zayas and C. A. Terrero-Escalante, “Black Holes in Cascading Theories: Confinement/Deconfinement Transition and other Thermal Properties,” *JHEP* **0709** (2007) 083 [arXiv:0707.2737 [hep-th]].
- [14] S. B. Giddings, “High energy QCD scattering, the shape of gravity on an IR brane, and the Froissart bound,” *Phys. Rev. D* **67** (2003) 126001 [arXiv:hep-th/0203004].
- [15] M. Krasnitz, “A two point function in a cascading $N = 1$ gauge theory from supergravity,” arXiv:hep-th/0011179.
- [16] E. Caceres and R. Hernandez, “Glueball masses for the deformed conifold theory,” *Phys. Lett. B* **504** (2001) 64 [arXiv:hep-th/0011204].
- [17] X. Amador and E. Caceres, “Spin two glueball mass and glueball Regge trajectory from supergravity,” *JHEP* **0411** (2004) 022 [arXiv:hep-th/0402061].
- [18] H. Firouzjahi and S. H. Tye, “The shape of gravity in a warped deformed conifold,” *JHEP* **0601**, 136 (2006) [arXiv:hep-th/0512076].
- [19] T. Noguchi, M. Yamaguchi and M. Yamashita, “Gravitational Kaluza-Klein modes in warped superstring compactification,” *Phys. Lett. B* **636**, 221 (2006) [arXiv:hep-th/0512249].
- [20] A. Y. Dymarsky and D. G. Melnikov, “On the glueball spectrum in the Klebanov-Strassler model,” *JETP Lett.* **84** (2006) 368 [*Pisma Zh. Eksp. Teor. Fiz.* **84** (2006) 440].

- [21] M. Berg, M. Haack and W. Mueck, “Glueballs vs. gluinoballs: Fluctuation spectra in non-AdS/non-CFT,” arXiv:hep-th/0612224.
- [22] A. Dymarsky and D. Melnikov, “Gravity Multiplet on KS and BB Backgrounds,” arXiv:0710.4517 [hep-th].
- [23] M. K. Benna, A. Dymarsky, I. R. Klebanov and A. Solovoyov, “On Normal Modes of a Warped Throat,” arXiv:0712.4404 [hep-th].
- [24] L. Kofman and P. Yi, “Reheating the universe after string theory inflation,” Phys. Rev. D **72** (2005) 106001 [arXiv:hep-th/0507257].
- [25] O. Aharony, Y. E. Antebi and M. Berkooz, “Open string moduli in KKLТ compactifications,” Phys. Rev. D **72** (2005) 106009 [arXiv:hep-th/0508080].
- [26] A. Berndsen, J. M. Cline and H. Stoica, “Kaluza-Klein relics from warped reheating,” arXiv:0710.1299 [hep-th].
- [27] M. Srednicki, R. Watkins and K. A. Olive, “Calculations of relic densities in the early universe,” Nucl. Phys. B **310** (1988) 693.
- [28] C. Csaki, J. Erlich, T. J. Hollowood and Y. Shirman, “Universal aspects of gravity localized on thick branes,” Nucl. Phys. B **581** (2000) 309 [arXiv:hep-th/0001033].
- [29] B. Batell and T. Gherghetta, “Holographic Mixing Quantified,” Phys. Rev. D **76** (2007) 045017 [arXiv:0706.0890 [hep-th]].
- [30] S. B. Giddings and A. Maharana, “Dynamics of warped compactifications and the shape of the warped landscape,” Phys. Rev. D **73** (2006) 126003 [arXiv:hep-th/0507158].
- [31] A. R. Frey and A. Maharana, “Warped spectroscopy: Localization of frozen bulk modes,” JHEP **0608** (2006) 021 [arXiv:hep-th/0603233].
- [32] K. Benakli and A. Y. Smirnov, “Neutrino-modulino mixing,” Phys. Rev. Lett. **79** (1997) 4314 [arXiv:hep-ph/9703465].
- [33] G. D. Kribs and I. Z. Rothstein, “Bounds on long-lived relics from diffuse gamma ray observations,” Phys. Rev. D **55** (1997) 4435 [Erratum-ibid. D **56** (1997) 1822] [arXiv:hep-ph/9610468].
- [34] J. R. Ellis, G. B. Gelmini, J. L. Lopez, D. V. Nanopoulos and S. Sarkar, “Astrophysical Constraints On Massive Unstable Neutral Relic Particles,” Nucl. Phys. B **373** (1992) 399.
- [35] W. Buchmüller, L. Covi, K. Hamaguchi, A. Ibarra and T. Yanagida, “Gravitino dark matter in R-parity breaking vacua,” JHEP **0703** (2007) 037 [arXiv:hep-ph/0702184];
G. Bertone, W. Buchmüller, L. Covi and A. Ibarra, “Gamma-Rays from Decaying Dark Matter,” arXiv:0709.2299 [astro-ph].

- [36] F. Takayama and M. Yamaguchi, “Gravitino dark matter without R-parity,” *Phys. Lett. B* **485** (2000) 388 [arXiv:hep-ph/0005214];
 A. Ibarra and D. Tran, “Gamma Ray Spectrum from Gravitino Dark Matter Decay,” arXiv:0709.4593 [astro-ph];
 H. Yuksel and M. D. Kistler, “Dark Matter Might Decay... Just Not Today!,” arXiv:0711.2906 [astro-ph];
 S. Palomares-Ruiz, “Model-Independent Bound on the Dark Matter Lifetime,” arXiv:0712.1937 [astro-ph].
- [37] J. R. Hörandel, “The composition of cosmic rays at the knee,” *Nuovo Cim. B* **120** (2005) 825 [arXiv:astro-ph/0407554].
- [38] J. P. Conlon, F. Quevedo and K. Suruliz, “Large-volume flux compactifications: Moduli spectrum and D3/D7 soft supersymmetry breaking,” *JHEP* **0508** (2005) 007 [arXiv:hep-th/0505076];
 J. P. Conlon, S. S. Abdussalam, F. Quevedo and K. Suruliz, “Soft SUSY breaking terms for chiral matter in IIB string compactifications,” *JHEP* **0701** (2007) 032 [arXiv:hep-th/0610129];
 J. P. Conlon and F. Quevedo, “Astrophysical and Cosmological Implications of Large Volume String Compactifications,” *JCAP* **0708** (2007) 019 [arXiv:0705.3460 [hep-ph]].
- [39] M. Birkel and S. Sarkar, “Extremely high energy cosmic rays from relic particle decays,” *Astropart. Phys.* **9** (1998) 297 [arXiv:hep-ph/9804285];
 S. Sarkar and R. Toldra, “The high energy cosmic ray spectrum from massive particle decay,” *Nucl. Phys. B* **621**, 495 (2002) [arXiv:hep-ph/0108098].
- [40] A. Klemm, B. Lian, S. S. Roan and S. T. Yau, “Calabi-Yau fourfolds for M- and F-theory compactifications,” *Nucl. Phys. B* **518** (1998) 515 [arXiv:hep-th/9701023].
- [41] S. Kachru, R. Kallosh, A. Linde and S. P. Trivedi, “De Sitter vacua in string theory,” *Phys. Rev. D* **68** (2003) 046005 [arXiv:hep-th/0301240].
- [42] P. Candelas, A. Font, S. H. Katz and D. R. Morrison, “Mirror symmetry for two parameter models. 2,” *Nucl. Phys. B* **429** (1994) 626 [arXiv:hep-th/9403187];
 A. C. Avram, M. Kreuzer, M. Mandelberg and H. Skarke, “Searching for K3 fibrations,” *Nucl. Phys. B* **494** (1997) 567 [arXiv:hep-th/9610154];
 F. Denef, M. R. Douglas and B. Florea, “Building a better racetrack,” *JHEP* **0406** (2004) 034 [arXiv:hep-th/0404257].
- [43] M. Y. Khlopov and A. D. Linde, “Is It Easy To Save The Gravitino?,” *Phys. Lett. B* **138** (1984) 265;
 I. V. Falomkin, G. B. Pontecorvo, M. G. Sapochnikov, M. Y. Khlopov, F. Balestra and G. Piragino, “Low-Energy Anti-P He-4 Annihilation And Problems Of The Modern Cosmology, GUT And Susy Models,” *Nuovo Cim. A* **79** (1984) 193 [*Yad. Fiz.* **39** (1984) 990];

- M. Y. Khlopov, Yu. L. Levitan, E. V. Sedelnikov and I. M. Sobol, “Nonequilibrium cosmological nucleosynthesis of light elements: Calculations by the Monte Carlo method,” *Phys. Atom. Nucl.* **57** (1994) 1393 [*Yad. Fiz.* **57** (1994) 1466];
R. H. Cyburt, J. R. Ellis, B. D. Fields and K. A. Olive, “Updated nucleosynthesis constraints on unstable relic particles,” *Phys. Rev. D* **67** (2003) 103521 [arXiv:astro-ph/0211258].
- [44] M. Kawasaki, K. Kohri and T. Moroi, “Big-bang nucleosynthesis and hadronic decay of long-lived massive particles,” *Phys. Rev. D* **71** (2005) 083502 [arXiv:astro-ph/0408426].
- [45] F. Brümmer, A. Hebecker and E. Trincherini, “The throat as a Randall-Sundrum model with Goldberger-Wise stabilization,” *Nucl. Phys. B* **738** (2006) 283 [arXiv:hep-th/0510113].
- [46] L. Randall and R. Sundrum, “Out of this world supersymmetry breaking,” *Nucl. Phys. B* **557** (1999) 79 [arXiv:hep-th/9810155].
- [47] F. Brümmer, A. Hebecker and M. Trapletti, “SUSY breaking mediation by throat fields,” *Nucl. Phys. B* **755** (2006) 186 [arXiv:hep-th/0605232].
- [48] K. Choi and K. S. Jeong, “Supersymmetry breaking and moduli stabilization with anomalous U(1) gauge symmetry,” *JHEP* **0608** (2006) 007 [arXiv:hep-th/0605108].
- [49] S. Kachru, L. McAllister and R. Sundrum, “Sequestering in string theory,” *JHEP* **0710** (2007) 013 [arXiv:hep-th/0703105].